Article (refereed) - postprint

Dennis, Emily B.; Morgan, Byron J.T.; Freeman, Stephen N.; Roy, David B.; Brereton, Tom. 2016. **Dynamic models for longitudinal butterfly data**. *Journal of Agricultural, Biological, and Environmental Statistics*, 21 (1). 1-21. 10.1007/s13253-015-0216-3

Dynamic models for longitudinal butterfly data

Abstract

We present models which provide succinct descriptions of longitudinal seasonal insect count data. This approach produces, for the first time, estimates of the key parameters of brood productivities. It may be applied to univoltine and bivoltine species. For the latter, the productivities of each brood are estimated separately, which results in new indices indicating the contributions from different generations.

The models are based on discrete distributions, with expectations that reflect the underlying nature of seasonal data. Productivities are included in a deterministic, auto-regressive manner, making the data from each brood a function of those in the previous brood. A concentrated likelihood results in appreciable efficiency gains. Both phenomenological and mechanistic models are used, including weather and site-specific covariates.

Illustrations are provided using data from the UK Butterfly Monitoring Scheme, however the approach is perfectly general. Consistent associations are found when estimates of productivity are regressed on northing and temperature. For instance, for univoltine species productivity is usually lower following milder winters, and mean emergence times of adults for all species have become earlier over time, due to climate change.

The predictions of fitted dynamic models have the potential to improve understanding of fundamental demographic processes. This is important for insects such as UK butterflies, many species of which are in decline.

Supplementary materials for this article are available online.

KEYWORDS: abundance indices; auto-regression; concentrated likelihood; generalised additive models; phenology; stopover models

1. INTRODUCTION

Climate change is predicted to become an increasingly important cause of biodiversity decline (Thomas et al., 2004; Pereira et al., 2010). Species' responses to climate are often complex and present challenges for modelling and prediction. We illustrate the models of this paper with reference to butterflies, the most comprehensively monitored insects. Their population status is increasingly recognised as an indicator for changes in biodiversity as they respond sensitively and rapidly to changes in habitat and climate (Thomas, 2005).

Previous studies of UK butterflies imply positive associations of populations with warm summer weather, but predicted relationships with winter weather are variable (Roy et al., 2001; Dennis and Sparks, 2007; Isaac et al., 2011). Evidence for shifts in phenology (Roy and Sparks, 2000) and increases in voltinism (Altermatt, 2010) have also been presented.

Extensive sources of citizen-science count data for butterflies are available both in the UK and around the world and there is much interest in developing robust modelling approaches to assist the monitoring and understanding of species' responses to change. Butterflies have multi-stage life cycles, and counts fluctuate within each year in response to their emergence as adults, which is generally the only life stage with widespread data. Soulsby and Thomas (2012) developed a mathematical model for this variation, but only allowed for discrete, non-overlapping generations. Other models have been proposed to describe the within-year variation, both non-parametrically using generalised additive models (GAMs, Rothery and Roy, 2001; Dennis et al., 2013) and via stochastic mixture models (Matechou et al., 2014; TR). Counts adjusted for seasonal fluctuations can then be used to produce longer-term trends, but existing methods do not impose any relationship between counts from one year to the next, which is the topic of this paper.

Causes of variation in both abundance and seasonal pattern from one year to the next are multi-faceted, relating to numbers during the previous year, as well as other factors driving the unobserved stages of the life-cycle, such as weather. We describe a novel dynamic framework which models count data across multiple sites from consecutive years, with

abundance in any given year driven by that in the previous year. We adapt the approach for bivoltine species, with the first brood in a year feeding into the second. The models can be fitted efficiently using concentrated likelihoods. Performance is illustrated for a sample of species, making comparisons with indices generated from GAMs, and introducing new methods of exploring covariate dependence.

Although we present and illustrate the work in terms of butterflies, it may be applied to other insect species, possibly after modification appropriate to their ecology. For example, the flightless longhorn beetle, *Dorcadion fuliginator*, takes two years to reach maturity (Baur et al., 2005), as do many dragonflies and some crickets. The models may also be adapted for the study of migrant bird populations.

2. MATERIALS AND METHODS

For any species, suppose counts of adults are recorded at S sites, each visited on up to T occasions, in each of Y successive years. Each can be treated as the realisation of a random variable from a suitable discrete distribution. For example, if this is taken as Poisson, with expectation $\lambda_{i,j,k}$ for site i, visit j, and year k, the likelihood has the form

$$\mathrm{L}(\boldsymbol{\rho}, \boldsymbol{\mu}, \boldsymbol{\sigma}, \boldsymbol{N}_1; \boldsymbol{y}) = \prod_{i=1}^{S} \prod_{j=1}^{T} \prod_{k=1}^{Y} \frac{\exp(-\lambda_{i,j,k}) \lambda_{i,j,k}^{y_{i,j,k}}}{y_{i,j,k}!},$$

where $\{y_{i,j,k}\}$ are the counts and $\boldsymbol{\rho}$, $\boldsymbol{\mu}$, $\boldsymbol{\sigma}$ and $\boldsymbol{N}_1$, are the model parameters which we describe in the next sections.

We adopt the Poisson distribution throughout, but there are other possibilities, such as negative-binomial or zero-inflated Poisson, for which an approximate concentrated likelihood approach is possible (TR). Alternatively, Pagel et al. (2014) accounted for overdispersion with respect to this simple model by a mixed log-normal-Poisson distribution.

The methods of the paper provide joint modelling of data obtained at different temporal scales. We consider two model types which are structurally different: a phenomenological model based simply on normal probability density functions and mechanistic models that are

based upon stopover models, which involve mechanisms allowing for estimation of survival.

2.1 Phenomenological model for univoltine species

For a univoltine species the counts within a season increase from zero and then decrease to zero corresponding to the emergence and death of adult butterflies. This variation may be described by Normal probability density $\mathrm{N}(\mu_{i,k}, \sigma^2_{i,k})$, corresponding to site i and year k, so that for the jth visit at time $t_{i,j,k}$ (e.g. week number in the season) we have

$$\lambda_{i,j,k} = N_{i,k} \frac{1}{\sigma_{i,k}\sqrt{2\pi}} \exp\left\{ -\frac{(t_{i,j,k} - \mu_{i,k})^2}{2\sigma^2_{i,k}} \right\}, \tag{1}$$

which we write as $\lambda_{i,j,k} = N_{i,k} a_{i,j,k}$, where $N_{i,k}$ provides an estimate of relative abundance for site i in a given year, k, and $\{a_{i,j,k}\}$ describes the seasonal variation over visits within that year. Thus for site i and year k the counts for any visit have a Poisson distribution with mean value proportional to the Normal probability density function centred on $\mu_{i,k}$.

We allow the relative abundance $N_{i,k+1}$, for site i and year $k+1$, to depend upon that in the previous year, $N_{i,k}$, in a deterministic first-order autoregressive manner via a growth rate, $\rho_{i,k}$ which, assuming the species does not overwinter as an adult (in which case a model for multiple generations is required), we define as "productivity", i.e. $N_{i,k+1} = \rho_{i,k} N_{i,k}$. Developing this recursion over time provides

$$\lambda_{i,j,1} = N_{i,1} a_{i,j,1} \quad \text{and} \quad \lambda_{i,j,k} = N_{i,k} a_{i,j,k} = \left(N_{i,1} \prod_{m=1}^{k-1} \rho_{i,m} \right) a_{i,j,k} \quad \text{for } k > 1, \tag{2}$$

which is similar to the model in Freeman and Newson (2008), but with a seasonal component. The productivities, $\{\rho_{i,k}\}$, describe the successes of a given generation over sites (i) for each year (k) and represent products of the number of eggs laid per adult and the probability of each egg reaching the adult stage in the next generation. The expressions of equation (2) characterise the univoltine models of the paper, with different formulations for the seasonal pattern, $\{a_{i,j,k}\}$, providing different models, as we shall see for a mechanistic model

formulation in Section 2.3.

2.2 Phenomenological model for bivoltine species

Bivoltine butterfly species have two broods each year, with the adults of the second brood arising from the eggs laid by the adults of the first. We may extend the model above to describe counts from two annual broods by incorporating two Normal distributions in the model for $\lambda_{i,j,k}$. Thus we set

$$\lambda_{i,j,k} = N_{i,k,1}\frac{1}{\sigma_{i,k,1}\sqrt{2\pi}}\exp\left\{-\frac{(t_{i,j,k}-\mu_{i,k,1})^2}{2\sigma^2_{i,k,1}}\right\} + N_{i,k,2}\frac{1}{\sigma_{i,k,2}\sqrt{2\pi}}\exp\left\{-\frac{(t_{i,j,k}-\mu_{i,k,2})^2}{2\sigma^2_{i,k,2}}\right\},$$

which we may write as

$$\lambda_{i,j,k} \equiv N_{i,k,1}a_{i,j,k,1} + N_{i,k,2}a_{i,j,k,2},$$

where at site i in year k the relative abundance for the first brood is given by $N_{i,k,1}$ and for the second brood by $N_{i,k,2}$. For the means and variances of the two Normal densities the final subscripts designate brood, and we have $\mu_{i,k,2} > \mu_{i,k,1}$.

Whereas in TR two broods are described by a mixture of probability density functions, here the relative abundance of a second brood in each year is assumed to depend on that of the first brood that year. Dependence between the two broods in any year is introduced by defining

$$N_{i,k,2} = \rho_{i,k,1}N_{i,k,1},$$

in addition to the between-year dependence, now given by

$$N_{i,k+1,1} = \rho_{i,k,2}N_{i,k,2}.$$

Thus $\rho_{i,k,1}$ represents the productivity of the first brood in a given year k, and $\rho_{i,k,2}$ represents the productivity of the second brood, which feeds into the relative abundance of the first

brood of the following year, $N_{i,k+1,1}$. So developing the recursion over time we write

$$\begin{aligned}\lambda_{i,j,1} &= N_{i,1,1}a_{i,j,1,1} + N_{i,1,2}a_{i,j,1,2} \\ &= N_{i,1,1}(a_{i,j,1,1} + \rho_{i,1,1}a_{i,j,1,2}),\end{aligned} \tag{3}$$

and

$$\begin{aligned}\lambda_{i,j,k} &= N_{i,k,1}a_{i,j,k,1} + N_{i,k,2}a_{i,j,k,2} \\ &= \left(N_{i,1,1}\prod_{m=1}^{k-1}\prod_{b=1}^{2}\rho_{i,m,b}\right)a_{i,j,k,1} + \left(N_{i,1,1}\rho_{i,k,1}\prod_{m=1}^{k-1}\prod_{b=1}^{2}\rho_{i,m,b}\right)a_{i,j,k,2} \\ &= N_{i,1,1}\left(a_{i,j,k,1} + \rho_{i,k,1}a_{i,j,k,2}\right)\prod_{m=1}^{k-1}\prod_{b=1}^{2}\rho_{i,m,b} \quad \text{for } k > 1.\end{aligned} \tag{4}$$

The extension to multivoltine species, with greater than two broods each year is immediate, though not greatly applicable to UK species. The new development for bivoltine/ multivoltine species is naturally based on the fact that the relative size of a given brood depends on the productivity of the previous brood. Notationally we denote the phenomenological models by P_B, where B is the number of broods.

2.3 Mechanistic and stopover models

Relatively little is known regarding butterfly survival, and what is known results from local short-term mark-recapture programs, which are expensive. To build survival into our models we introduce additional parameters, the emergence times of adults, which are typically unknown and of interest in their own right as indicators of phenological change in a specific, key point in a species' life-cycle. We do this as follows.

Suppose first of all that there is only one brood, and a site abundance $N_{i,k}$ for site i and year k. In order to describe the emergence times we introduce parameters $\beta_{i,d-1,k}$, which describe the proportions of $N_{i,k}$ emerging at site i and just prior to visit d in year k. The

expected number of individuals at site i at time $t_{i,j,k}$ in year k is given as

$$\lambda_{i,j,k} = N_{i,k} a_{i,j,k} = N_{i,k} \left\{ \sum_{d=1}^{j} \beta_{i,d-1,k} \left(\prod_{m=d}^{j-1} \phi_{i,m,k} \right) \right\}, \tag{5}$$

where the index $d = 1, \ldots, j$ indicates the possible times of emergence for an individual detected on visit j. The parameters $\beta_{i,d-1,k}$ describe the proportions of $N_{i,k}$ emerging at site i and visit d in year k, such that $\sum_{d=1}^{T} \beta_{i,d-1,k} = 1$, for each site i and year k. We define $\phi_{i,m,k}$ as the probability that an individual that is present at site i at visit m in year k, will remain at that site until visit $m+1$. So for example, $\lambda_{i,3,k} = N_{i,k} \left(\beta_{i,0,k} \phi_{i,1,k} \phi_{i,2,k} + \beta_{i,1,k} \phi_{i,2,k} + \beta_{i,2,k} \right)$.

In order that the emergence parameters have the right type of shape we can set

$$\beta_{i,d-1,k} = F_{i,k}(t_{i,d,k}) - F_{i,k}(t_{i,d,k} - 1), \tag{6}$$

where $F_{i,k}(t_{i,d,k}) = P(X \leq t_{i,d,k})$ for $X \sim N(\mu_{i,k}, \sigma^2_{i,k})$, where $\mu_{i,k}$ is the mean date of emergence and $\sigma^2_{i,k}$ is the associated variance. For each i, k, $\beta_{i,0,k} = F_{i,k}(1)$ and $\beta_{i,T-1,k} = 1 - F_{i,k}(T-1)$.

This is a simple stopover model, proposed for butterfly data by Matechou et al. (2014); see also TR. Stopover models are used in describing data on migrating birds, which rest and feed during their journey at particular stopover sites where observations take place. Typically, the resulting counts, graphed over time, reflect successive waves of birds arriving, staying and then leaving. Matechou et al. (2014) observe that this is the same pattern seen when adult butterflies are counted within a season, with for example bivoltine species analogous to two waves of birds observed at a stopover site.

In Matechou et al. (2014) the above model is extended to account for multivoltine data, and the expression of equation (6) then becomes a mixture of terms, each of which is an area under an appropriate probability density function. In the multivoltine case we need a different dynamic mechanistic model, in order to allow for the abundance of one brood to feed into that of a succeeding brood, during the same year.

In the univoltine dynamic stopover model, the recursions of equation (2) apply, but now with the different specification of $\{a_{i,j,k}\}$ provided by equation (5). For the multivoltine case in the dynamic mechanistic model we assign a separate site abundance to each brood in a year. Thus we assume the two broods for bivoltine species to be separate such that, for site i, visit j and brood b, in year k, we extend equation (5) to give

$$a_{i,j,k,b} = \sum_{d=1}^{j} \beta_{i,d-1,k,b} \left(\prod_{m=d}^{j-1} \phi_{i,d,k,b} \right), \quad \text{for } b = 1, 2, \tag{7}$$

where we define $\{\phi_{i,d,k,b}\}$ as the appropriate survival probabilities of an individual from one visit to the next, which are now estimated separately for each brood. This development is an extension of that in the original specficiation of Matechou et al. (2014). For brood b, the parameters $\{\beta_{i,d-1,k,b}\}$ describe the proportions of $N_{i,k,b}$ arriving at visit d, and are modelled here using Normal distributions, so that

$$\beta_{i,d-1,k,b} = F_{i,k,b}(t_{i,d,k}) - F_{i,k,b}(t_{i,d,k} - 1),$$

where $F_{i,k,b}(t_{i,d,k}) = \Pr(X \leq t_{i,d,k})$, for $X \sim N(\mu_{i,k,b}, \sigma^2_{i,k,b})$, and $\mu_{i,k,b}$ is the appropriate mean date of emergence of adults for brood b and $\sigma^2_{i,k,b}$ is the corresponding variance. For each i, k, and b, $\beta_{i,0,k,b} = F_{i,k,b}(1)$ and $\beta_{i,T-1,k,b} = 1 - F_{i,k,b}(T-1)$. The recursions of equations (3) and (4) then apply, but now with the new specification of $\{a_{i,j,k,b}\}$ from equation (7). Notationally we specify the dynamic mechanistic model by M_B, where B is the number of broods.

2.4 Concentrated likelihood

We fit models to data by maximum likelihood. As in TR, the number of parameters in the likelihood can be reduced by S, using a concentrated likelihood approach. S is typically large for these models and so computational efficiency is substantially increased. We consider first the univoltine case. Using equation (2), apart from an additive constant, the log-likelihood

for site i may be written as

$$\ell_i = \mathrm{Log}(\mathrm{L}_i) = \sum_{j=1}^{T} \Bigg[-N_{i,1} a_{i,j,1} + y_{i,j,1} \log\left(N_{i,1} a_{i,j,1}\right) + \sum_{k=2}^{Y} \left\{ -N_{i,1} a_{i,j,1} \prod_{m=1}^{k-1} \rho_{i,m} + y_{i,j,k} \log\left(N_{i,1} a_{i,j,k} \prod_{m=1}^{k-1} \rho_{i,m} \right) \right\} \Bigg]. \quad (8)$$

For the data from all sites the log-likelihood is $\ell = \sum_{i=1}^{S} \ell_i$. Using equation (8) we obtain

$$\frac{\partial \ell}{\partial N_{i,1}} = \sum_{j=1}^{T} \left\{ -a_{i,j,1} + \frac{y_{i,j,1}}{N_{i,1}} + \sum_{k=2}^{Y} \left(-a_{i,j,1} \prod_{m=1}^{k-1} \rho_{i,m} + \frac{y_{i,j,k}}{N_{i,1}} \right) \right\},$$

and equating to zero we find

$$N_{i,1} = \sum_{j=1}^{T} \frac{\sum_{k=1}^{Y} y_{i,j,k}}{a_{i,j,1} + \sum_{k=2}^{Y} a_{i,j,k} \prod_{m=1}^{k-1} \rho_{i,m}}. \quad (9)$$

We note how $N_{i,1}$ is a weighted sum over visits of totals at site i across years. Thus despite an apparent strong dependence of $\{N_{i,k}\}$ on $\{N_{i,1}\}$ in (2), this is only a consequence of the deterministic links between the $\{N_{i,k}\}$, and all data contribute to the estimation of $\{N_{i,1}\}$, and hence $\{N_{i,k}\}$. Substitution of the expressions for $\{N_{i,1}\}$ from (9) in (8) results in a concentrated likelihood, which is maximised with respect to only the parameters associated with $\boldsymbol{\rho}$ and $\mathbf{a}$ (which contain the elements of $\boldsymbol{\mu}$ and $\boldsymbol{\sigma}$). Estimation of $\{N_{i,1}\}$ is then made by substituting estimates of $\{a_{i,j,k}\}$ and $\{\rho_{i,m}\}$ into (9). The above approach holds for both phenomenological and mechanistic models.

The concentrated likelihood for the bivoltine case is given similarly in Appendix A. We maximise the concentrated likelihoods using the `optim` function in `R` (R Core Team, 2015), with the limited-memory BFGS algorithm (Byrd et al., 1995). Associated `R` code for the dynamic models is provided in the Supporting Information.

2.5 Annual index of abundance

In the following we write $\widehat{\theta}$ for the maximum-likelihood estimate of θ, for any parameter θ. The averages of the relative site abundance estimates, for each year k, are used to create an index of abundance G_k for year k. For a univoltine species we set

$$G_k = \frac{1}{S}\sum_{i=1}^{S}\widehat{N}_{i,k} = \begin{cases} \dfrac{1}{S}\displaystyle\sum_{i=1}^{S}\widehat{N}_{i,1} & \text{if } k = 1 \\ \dfrac{1}{S}\displaystyle\sum_{i=1}^{S}\left(\widehat{N}_{i,1}\prod_{m=1}^{k-1}\widehat{\rho}_{i,m}\right) & \text{if } k > 1, \end{cases} \tag{10}$$

for $k = 1, \ldots, Y$, from equations (2). Similarly for the bivoltine case we estimate an index $G_{k,b}$ for each brood, $b = 1, 2$, as

$$G_{k,1} = \frac{1}{S}\sum_{i=1}^{S}\widehat{N}_{i,k,1} = \begin{cases} \dfrac{1}{S}\displaystyle\sum_{i=1}^{S}\widehat{N}_{i,1,1} & \text{if } k = 1 \\ \dfrac{1}{S}\displaystyle\sum_{i=1}^{S}\left(\widehat{N}_{i,1,1}\prod_{m=1}^{k-1}\prod_{b=1}^{2}\widehat{\rho}_{i,m,b}\right) & \text{if } k > 1, \end{cases} \tag{11}$$

and

$$G_{k,2} = \frac{1}{S}\sum_{i=1}^{S}\widehat{N}_{i,k,2} = \begin{cases} \dfrac{1}{S}\displaystyle\sum_{i=1}^{S}\widehat{N}_{i,1,1}\widehat{\rho}_{i,k,1} & \text{if } k = 1 \\ \dfrac{1}{S}\displaystyle\sum_{i=1}^{S}\left(\widehat{N}_{i,1,1}\widehat{\rho}_{i,k,1}\prod_{m=1}^{k-1}\prod_{b=1}^{2}\widehat{\rho}_{i,m,b}\right) & \text{if } k > 1, \end{cases} \tag{12}$$

for $k = 1, \ldots, Y$, making use of the recursions demonstrated in equations (3) and (4). The separate brood indices can be added to produce a single, annual index but there is potentially great ecological benefit in maintaining them separately, as each corresponds to different times of year and may be driven by different environmental factors.

Once indices are formed they are plotted against year, and we shall see examples in Section 3. Standard errors for the indices can be obtained via bootstrapping, as for other methods (Dennis et al., 2013; TR). Error bars are not presented here for clarity, but in general the differences between the indices derived from the dynamic models and alternative methods (which we explore in the next section), are smaller than the size of the errors.

2.6 Application

We apply the dynamic models to national monitoring scheme data for a subset of UK butterfly species. The UK Butterfly Monitoring Scheme (UKBMS) is the primary source of count data for UK butterflies. The scheme relies on recorders who count butterflies under favorable conditions each week between early April and late September, the main period for butterfly activity. This results in a maximum of $T = 26$ each year, though typically not all of the 26 designated visits are made, so the data do not need to be equally spaced. The UKBMS has grown gradually since it began in 1976 to over 1100 sites monitored in 2012 (Botham et al., 2013). Population trends are typically calculated annually for 56 of the 59 butterfly species regularly found in the UK.

Many studies of UKBMS data involve application to a single illustrative species (Matechou et al., 2014; Pagel et al., 2014). We demonstrate the dynamic models with application to a sample of representative, taxonomically and ecologically diverse species. Six univoltine and five bivoltine species were selected, with varying range size, habitat requirements and phenologies, although very scarce, habitat-specialist species, which generally have limited data, were not considered in this analysis. Each model was fitted to data for 1978-2011. The UK butterfly transect data used in this study are archived by the UKBMS (http://www.ukbms.org).

Sites at which the species of interest was never recorded or at which monitoring was undertaken for fewer than five years were excluded from this analysis. For illustration, a subset of 100 monitored sites was randomly selected for each species, with the exception of Holly Blue, for which a sample of up to 200 sites was instead taken, since using only 100 sites produced bias in the estimates of productivity.

We illustrate the performance of the dynamic models in terms of abundance indices, productivity, survival and phenology. Additional figures and tables are given in Appendix S1 of the Supporting Information. This will be done for the samples of the univoltine and bivoltine species, with and without the addition of covariates. Where parameters were

assumed to be constant spatially the subscript for site, i, is omitted. In models for bivoltine species, we let $\mu_2 = \mu_1 + \mu_d$, where $\mu_1 \geq 0$ and $\mu_d > 0$, to ensure that $\mu_2 > \mu_1$.

The covariates we select are northing and measures of temperature. They were chosen to demonstrate the potential of the models, and may not be optimal. All covariates were standardised to have zero mean and unit variance. We use monthly mean and minimum Central England Temperature data (Parker et al., 1992).

The average minimum daily temperature during October-March was used as a covariate for overwinter productivity. For bivoltine species, the mean temperature within the flight period of the first brood was used to describe productivity of the first brood. Productivities, which are necessarily positive, were regressed on the log scale. Survival in mechanistic models was logistically regressed on mean temperature within the flight period of the brood of interest. Scientific names and approximate flight periods for the species studied are provided in Table S1.1, and the latter were used to indicate the relevant temperature covariates. Due to interest in the possible effect of covariates on estimates of survival, we primarily use mechanistic models when covariates are employed and phenomenological models otherwise, however alternatives are also possible.

3. RESULTS

3.1 Indices

Indices of abundance are derived from estimates of annual productivity and estimates of initial abundance from the dynamic model, as described in Section 2.5. Here μ and σ have been considered constant, although varying these between years provides useful information and we shall see examples of this later, but it had no distinguishable effect on indices of abundance. We compare relative abundance indices for model P_1 and an approach with GAM-based models for seasonal patterns, currently adopted by the UKBMS and described by Dennis et al. (2013). To compare the different indices, each index was standardised to have zero mean and unit variance. An additional comparison with the

generalised abundance index (GAI) approach (TR) and consideration of goodness-of-fit are given in Appendix S2 of the Supporting Information.

The fitted phenomenological dynamic models discussed in the context of indices have 35 and 71 parameters for $B = 1, 2$, respectively. Given that $Y = 34$, in the univoltine case there are 33 annual estimates ρ_k, as well as μ and σ, and in the bivoltine case, there are 34 parameters $\rho_{k,1}$ and 33 parameters $\rho_{k,2}$, in addition to μ_1, μ_d, σ_1 and σ_2.

Figure 1a) gives a comparison between annual indices of abundance for six univoltine species. There is good agreement between the indices resulting from the dynamic model and the standard GAM approach (Dennis et al., 2013). By estimating an index for each brood (equations 11 and 12), dynamic models P_2 allow us to add more information to indices for bivoltine species, which we illustrate in two different ways in Figures 2a) and S1.1. We see how the dynamic model allows us to elaborate the indices produced by the GAM approach, by providing a separate index for each brood in the bivoltine case. This could, for example, reveal differing trends between broods.

For model verification, Appendix S3 of the Supporting Information summarises the results of applying the dynamic models to simulated data.

3.2 Productivity

Figure 1b) presents estimates of productivity for the univoltine species, from fitting model P_1. Values of $\rho_{k,}$ greater than unity indicate growth compared to the previous year, and values less than unity indicate decline. Hence as anticipated we see a tendency for productivities less than unity for species in decline, such as Small Skipper in recent years, while for Marbled White productivities tend to be above unity during the initial period of growth, followed by recent fluctuations about unity, when the population appears to be relatively stable.

Figure 2b) presents estimated productivities for each brood for five bivoltine species, using model P_2. Values above/below unity represent growth/decline relative to the previous brood. In Figure S1.2 we see how the productivities reflect the relative sizes of the fitted

seasonal curves, for which the average over the series is shown (standardised to sum to unity). The relative sizes of the broods will actually vary with productivity each year.

Figure 3 shows the results of including covariates in the dynamic models, in this case for model M_1 with $\rho_{i,k}$ and $\phi_{i,k}$ (which we revisit in Section 3.3) varying with temperature and northing. It is interesting that with the exception of Gatekeeper, higher productivity is significantly associated with cooler winters and in all cases with more Northerly latitudes (regression coefficients and associated standard errors are presented in Table S1.2a).

Figure 4 shows the effect of adding covariates for bivoltine species, in this case for model M_2 with productivity varying with temperature and northing, and survival varying with temperature, which we discuss further in Section 3.3. As detailed in Section 2.6, first brood productivity was associated with the mean temperature during the first brood, and second brood productivity with the minimum winter overwinter temperture. Associations of first-brood productivity, $\rho_{i,k,1}$, with northing and weather varied between species, and regression coefficients for the slope parameters were generally significant (Table S1.3a). The association of higher productivity with cooler winters shown for univoltine species is also found for the second brood of the bivoltine species, with the exception of Wall Brown and Holly Blue, which is a common garden visitor, unlike the other species which favour grasslands, as well as gardens in the case of Small White and Green-veined White.

Given an estimate of productivity for each year, if desired the geometric mean of the productivities over time may be used to provide a simple comparison between species.

3.3 Survival

The mechanistic models allow estimation of the survival probabilities, ϕ, of butterflies, from which adult life expectancies (in weeks) can be estimated by $1/(1-\phi)$, assuming that a species does not overwinter as an adult. Variation in life expectancy with temperature is displayed for univoltine species in Figure S1.3, and for bivoltine species in Figure S1.4, based on the models fitted with covariates in the previous section. Tables S1.2 and S1.3 show the parameter estimates and associated standard errors from the M_B models with covariates.

For comparison estimates are also included for the P_1 and P_2 models with covariates for ρ, which are not presented in the figures, but produce analogous estimates of the shared parameters. There are differences in μ and σ since in the mechanistic model μ represents the mean date of emergence which will be earlier than the mean flight date, and σ relates to the length of the period of emergence, which will be shorter than the length of the flight period in the P_1 model. The associated errors for μ and σ are smaller for the P_1 than for the M_1 model. For the bivoltine species there is more variation in the estimates from P_2 and M_2. As in the univoltine case, standard errors from the phenomenological model tend to be smaller than those from the mechanistic model. The M_B models with covariates have 8 and 14 parameters for $B = 1, 2$, respectively, compared to the P_B models with 5 and 10 parameters for $B = 1, 2$, respectively. In these cases reduced precision is a consequence of greater model complexity.

For univoltine species, there was a significant negative association of life expectancy with higher average temperature during the flight period for four out of six species (Figure S1.3 and Table S1.2a). Four univoltine species indicated significantly greater survival at southerly sites. Standard errors in Table S1.2a) are generally small, but are large for two instances for Green Hairstreak, which exhibit flatness in the associated plots (Figures 3 and S1.3).

As for the associations of first brood productivity with weather, in bivoltine species we find that the variation in first brood life expectancy with temperature differs between the species sampled, and slope estimates were only significant for three out of five species (Table S1.3). With the exception of Holly Blue, life expectancy for the second brood of the bivoltine species increased significantly with temperature. Fitting model M_2 with covariates for northing and weather on ρ and ϕ for each brood produced unrealistic estimates of lifespan for Brown Argus and Holly Blue, hence in Figure S1.4 we allow ϕ in the M_2 model to vary with temperature and brood only. This requires further investigation, but is likely to be due to the relatively large number of parameters in model M_2 and/or relatively small size

of the sample. The corresponding standard errors for this model are sometimes large, for example, for Holly Blue (Table S1.3).

3.4 Phenology

Here we demonstrate the potential to produce estimates of phenology using the dynamic models. The P_1 and P_2 models were fitted with $\boldsymbol{\rho}$, $\boldsymbol{\mu}$ and $\boldsymbol{\sigma}$ each varying with year. Hence the P_1 model requires 101 parameters to be estimated, corresponding to 33 parameters for ρ_k, and 34 parameters each for μ_k and σ_k. Similarly the P_2 model has 203 parameters: 34 for $\rho_{k,1}$, 33 for $\rho_{k,2}$, and 34 each for $\mu_{k,1}$, $\mu_{k,d}$, $\sigma_{k,1}$ and $\sigma_{k,2}$. To identify potential phenological trends, the models were also fitted with the parameters of interest regressed upon year (indicated by blue lines), as in the models fitted to univoltine species for comparison with the GAI in Appendix S2 of the Supporting Information. We perform simple linear regressions post model-fitting to identify potential trends between μ and productivity ρ, where green lines indicate significant regressions (p-value > 0.05).

Figure 5 gives the mean and standard deviation of the flight periods for the univoltine species and corresponding figures for the bivoltine species are given in Figures S1.5 and S1.6. Figures 5a) and S1.5 suggest that the mean flight period date, μ, has advanced for all species and broods, which is consistent with what is expected under climate change (Sparks and Yates, 1997; Roy and Sparks, 2000). From Figures 5b) and S1.6 we see that the length of the flight period has generally increased, also in agreement with previous findings (Roy and Sparks, 2000). Table S2.1 suggests significant increases in σ for 5 out of 6 univoltine species. The location of the fitted line for the Marbled White σ_k in Figure 5b) is due to the increase in sample size over time giving more weight to the later years. Figures S1.5 and S1.6 show a small number of outliers which require further investigation.

With the exception of Green Hairstreak, for the six univoltine species there was no clear relationship between μ_k and ρ_k (Figure S1.7). For Green Hairstreak, which emerges early in the season, lower productivities are associated with an earlier flight period, which may lead to declines if advances in phenology continue with changes in climate. For most of the five

bivoltine species, significant patterns between the mean flight period for each generation and the associated productivity were not found (Figure S1.8). However for Brown Argus and Green-veined White, productivity of the second generation was lower when the mean flight period date of the second brood, $\mu_{k,2}$, was advanced.

These results show that the dynamic models predict phenological changes consistent with expected patterns. The dynamic models allow for improved estimates of phenology to be studied in combination with demographic parameters, to reveal potential novel insights. Changes in phenology may also be modelled using the mechanistic models, in order to separate changes in emergence time from changes in survival.

4. DISCUSSION

The dynamic model framework allows novel investigation of the drivers of fluctuations in abundance and provides a basis that can be adapted to both the study species and research aim. We have presented only a preliminary application. The methods of TR, which model data for each year separately, may be better suited for estimating indices of abundances efficiently (see Table S2.1), whereas dynamic models provide additional information of value for understanding demography. However the agreement of the indices obtained from the different methods provides confidence that the dynamic models are performing correctly, and that for multivoltine species indices may be derived separately for each brood.

For the majority of the sample species, higher overwinter productivity was associated with cooler winters, which may act to reduce the impact of pathogens. Variability in lifespan and first brood productivity of bivoltine species differed more between species. Given that species have different life-histories, further research may look for trait-based variation, for example overwintering stage: egg, larva, chrysalis or adult, all of which may be affected most severely by different environmental factors. For example, Diamond et al. (2011) explored relationships between changes in date of first appearance and species' traits.

Further work is needed to explore the relevant covariates driving changes in produc-

tivity, survival and phenology. Spatial covariates such as habitat/land-cover may describe additional variation in the parameters. Inclusion of local weather could identify the period within the life-cycle for which weather has the most impact on the adult stage. Growing degree-days may also be explored (Hodgson et al., 2011). In this study covariates were included additively on a logistic linear scale, whereas true relationships may be non-linear, for example productivity/survival might be limited by extremes in weather. The models could also be extended to model variation in productivity stochastically.

Alternatives to the Normal distribution for describing seasonal variation could be explored, for example to describe skewness (Calabrese, 2012). This study has only accounted for species which are distinctly univoltine or bivoltine. A spline may be used to define complex seasonal patterns (TR), and the models could be extended to allow more than two broods each year. The models may be developed to accommodate variation in voltinism, where the first generation contributes to both the second generation within the same year and first generation the following year, with relevance for study of potential "lost generations" (Van Dyck et al., 2015). The dynamic models may also be used to study species which aestivate under hot summer conditions (Spieth et al., 2011; Grill et al., 2013).

The dynamic models produce realistic estimates of parameters relevant to phenology, providing further validation of the models. Phenological studies have typically involved measures such as mean first encounter, mean peak encounter and mean length of the flight period (Roy and Sparks, 2000; Diamond et al., 2014; Karlsson, 2014), which may be driven by observer behaviour. The improved estimates of phenology from dynamic models provide the opportunity to study linkages between changes in phenology and changes in abundance and productivity, for example phenological mismatch (Hindle et al., 2015).

Using a phenomenological model may be optimal in scenarios with limited data, but the mechanistic model allows for additional insights by estimating survival. Spatio-temporal variation in the lifespans of butterflies has had limited attention, as have potential linkages with other parameters, for example to explore how phenology affects survival, or whether

variation in survival can influence productivity. Using a mechanistic model separates relevant parameters, for example to determine whether an increase in flight period length is due to an extended period of emergence, or increased lifespan. The model could be adapted to explore synchrony in populations (Powney et al., 2010), either between sites of a given species or across sites but between multiple species, by incorporating random effects (Lahoz-Monfort et al., 2011, 2013), for example in the ρ parameter for productivity. Density dependence, which has been highlighted for some butterflies (Nowicki et al., 2009), may be incorporated here in productivity and/or survival by introducing a dependency on the relative abundance. Additionally, allowing for spatial dependence of ρ and autocorrelation in abundance may be advantageous (Johnson et al., 2012). Pagel et al. (2014) included spatially autocorrelated random effects when modelling mean population density, but did not account for the within-year variability in counts.

For some threatened, conservation-priority UK butterflies, such as Large Blue, *Phengaris arion*, Brown Hairstreak *Thecla betulae*, and Marsh Fritillary, *Euphydryas aurinia*, data are available on other stages of the butterfly life-cycle, such as counts of caterpillars or eggs. An attraction of the model framework proposed is the potential for the incorporation of data from multiple stages of the life-cycle, which could aid the monitoring and conservation of rarer species for which coverage from standard monitoring schemes can be limited.

The dynamic models may address the "lack of mechanistic understanding about factors driving butterfly population dynamics" (Isaac et al., 2011). Future application will generate hypotheses for further investigation, with the potential to illuminate features of butterfly phenology and demography which are at present poorly understood.

APPENDIX A. CONCENTRATED LIKELIHOOD FOR BIVOLTINE SPECIES

Using equation (4), the log-likelihood for site i is given, apart from an additive constant, by

$$\begin{aligned}\ell_i = \mathrm{Log}(\mathrm{L}_i) = \sum_{j=1}^{T}\Bigg[& - N_{i,1,1}\left(a_{i,j,1,1} + \rho_{i,1,1}a_{i,j,1,2}\right) + y_{i,j,1}\log\left\{N_{i,1,1}\left(a_{i,j,1,1} + \rho_{i,1,1}a_{i,j,1,2}\right)\right\} \\ & + \sum_{k=2}^{Y}\Bigg\{-N_{i,1,1}\left(a_{i,j,k,1} + \rho_{i,k,1}a_{i,j,k,2}\right)\prod_{m=1}^{k-1}\prod_{b=1}^{2}\rho_{i,m,b} \\ & \qquad + y_{i,j,k}\log\left(N_{i,1,1}\left(a_{i,j,k,1} + \rho_{i,k,1}a_{i,j,k,2}\right)\prod_{m=1}^{k-1}\prod_{b=1}^{2}\rho_{i,m,b}\right)\Bigg\}\Bigg], \end{aligned} \tag{A.1}$$

where we have defined $\{a_{i,j,k,b}\}$ and $\{\rho_{i,k,b}\}$, for site i, visit j and brood b in year k in the previous sections. This gives

$$\begin{aligned}\frac{\partial \ell}{\partial N_{i,1,1}} = \sum_{j=1}^{T}\Bigg[& - \left(a_{i,j,1,1} + \rho_{i,1,1}a_{i,j,1,2}\right) + \frac{y_{i,j,1}}{N_{i,1,1}} \\ & + \sum_{k=2}^{Y}\Bigg\{-\left(a_{i,j,k,1} + \rho_{i,k,1}a_{i,j,k,2}\right)\prod_{m=1}^{k-1}\prod_{b=1}^{2}\rho_{i,m,b} + \frac{y_{i,j,k}}{N_{i,1,1}}\Bigg\}\Bigg],\end{aligned}$$

and equating to zero we find

$$N_{i,1,1} = \sum_{j=1}^{T}\frac{\sum_{k=1}^{Y} y_{i,j,k}}{a_{i,j,1,1} + \rho_{i,j,1}a_{i,j,1,2} + \sum_{k=2}^{Y}\left\{\left(a_{i,j,k,1} + \rho_{i,m,1}a_{i,j,k,2}\right)\prod_{m=1}^{k-1}\prod_{b=1}^{2}\rho_{i,m,b}\right\}}. \tag{A.2}$$

We note again how $N_{i,1,1}$ is a weighted sum over visits of totals at site i across years. As in the univoltine case, we substitute the expressions for $\{N_{i,1,1}\}$ from (A.2) into (A.1) and maximise the overall concentrated likelihood with respect to parameters associated with $\boldsymbol{\rho}$ and $\boldsymbol{a}$. Estimation of $\{N_{i,1,1}\}$ is obtained by substituting estimates of $\{a_{i,j,k,b}\}$ and $\{\rho_{i,k,b}\}$ into (A.2).

This concentrated likelihood approach applies for both the phenomenological and mechanistic models for bivoltine species, with variation only in the specification of $\{a_{i,j,k,b}\}$.

REFERENCES

Altermatt, F. (2010), "Climatic warming increases voltinism in european butterflies and moths", *Proceedings of the Royal Society B: Biological Sciences*, 277, 1281–1287.

Baur, B., Coray, A., Minoretti, N. and Zschokke, S. (2005), "Dispersal of the endangered flightless beetle *Dorcadion fuliginator* (Coleoptera: Cerambycidae) in spatially realistic landscapes", *Biological Conservation*, 124, 49–61.

Botham, M. S., Brereton, T. M., Middlebrook, I., Randle, Z. and Roy, D. B. (2013), United Kingdom Butterfly Monitoring Scheme report for 2012. Centre for Ecology & Hydrology, Wallingford.

Byrd, R. H., Lu, P., Nocedal, J. and Zhu, C. (1995), "A limited memory algorithm for bound constrained optimization", *SIAM Journal on Scientific Computing*, 16, 1190–1208.

Calabrese, J. M. (2012), "How emergence and death assumptions affect count-based estimates of butterfly abundance and lifespan", *Population Ecology*, 54, 431–442.

Dennis, E. B., Freeman, S. N., Brereton, T. and Roy, D. B. (2013), "Indexing butterfly abundance whilst accounting for missing counts and variability in seasonal pattern", *Methods in Ecology and Evolution*, 4, 637–645.

Dennis, R. L. H. and Sparks, T. H. (2007), "Climate signals are reflected in an 89 year series of British Lepidoptera records", *European Journal of Entomology*, 104, 763–767.

Diamond, S. E., Cayton, H., Wepprich, T., Jenkins, C. N., Dunn, R. R., Haddad, N. M. and Ries, L. (2014), "Unexpected phenological responses of butterflies to the interaction of urbanization and geographic temperature", *Ecology*, 95, 2613–2621.

Diamond, S. E., Frame, A. M., Martin, R. A. and Buckley, L. B. (2011), "Species' traits predict phenological responses to climate change in butterflies", *Ecology*, 92, 1005–1012.

Freeman, S. N. and Newson, S. E. (2008), "On a log-linear approach to detecting ecological interactions in monitored populations", *Ibis*, 150, 250–258.

Grill, A., Cerny, A. and Fiedler, K. (2013), "Hot summers, long life: egg laying strategies of Maniola butterflies are affected by geographic provenance rather than adult diet", *Contributions to Zoology*, 82, 27–36.

Hindle, B. J., Kerr, C. L., Richards, S. A. and Willis, S. G. (2015), "Topographical variation reduces phenological mismatch between a butterfly and its nectar source", *Journal of Insect Conservation*, 19, 227–236.

Hodgson, J. A., Thomas, C. D., Oliver, T. H., Anderson, B. J., Brereton, T. M. and Crone, E. E. (2011), "Predicting insect phenology across space and time", *Global Change Biology*, 17, 1289–1300.

Isaac, N. J. B., Girardello, M., Brereton, T. M. and Roy, D. B. (2011), "Butterfly abundance in a warming climate: patterns in space and time are not congruent", *Journal of Insect Conservation*, 15, 233–240.

Johnson, D. S., Conn, P., Hooten, M., Ray, J. and Pond, B. A. (2012), "Spatial occupancy models for large data sets", *Ecology*, 94, 801–808.

Karlsson, B. (2014), "Extended season for northern butterflies", *International Journal of Biometeorology*, 58, 691–701.

Lahoz-Monfort, J. J., Morgan, B. J. T., Harris, M. P., Daunt, F., Wanless, S. and Freeman, S. N. (2013), "Breeding together: modeling synchrony in productivity in a seabird community", *Ecology*, 94, 3–10.

Lahoz-Monfort, J. J., Morgan, B. J. T., Harris, M. P., Wanless, S. and Freeman, S. N. (2011), "A capture–recapture model for exploring multi-species synchrony in survival", *Methods in Ecology and Evolution*, 2, 116–124.

Matechou, E., Dennis, E. B., Freeman, S. N. and Brereton, T. (2014), "Monitoring abundance and phenology in (multivoltine) butterfly species: a novel mixture model", *Journal of Applied Ecology*, 51, 766–775.

Nowicki, P., Bonelli, S., Barbero, F. and Balletto, E. (2009), "Relative importance of

density-dependent regulation and environmental stochasticity for butterfly population dynamics", *Oecologia*, 161, 227–239.

Pagel, J., Anderson, B. J., O'Hara, R. B., Cramer, W., Fox, R., Jeltsch, F., Roy, D. B., Thomas, C. D. and Schurr, F. M. (2014), "Quantifying range-wide variation in population trends from local abundance surveys and widespread opportunistic occurrence records", *Methods in Ecology and Evolution*, 5, 751–760.

Parker, D. E., Legg, T. P. and Folland, C. K. (1992), "A new daily Central England Temperature series, 1772–1991", *International Journal of Climatology*, 12, 317–342.

Pereira, H. M., Leadley, P. W., Proença, V., Alkemade, R., Scharlemann, J. P., Fernandez-Manjarrés, J. F., Araújo, M. B., Balvanera, P., Biggs, R., Cheung, W. W. et al. (2010), "Scenarios for global biodiversity in the 21st century", *Science*, 330, 1496–1501.

Powney, G. D., Roy, D. B., Chapman, D. and Oliver, T. H. (2010), "Synchrony of butterfly populations across species' geographic ranges", *Oikos*, 119, 1690–1696.

R Core Team (2015), R: A language and environment for statistical computing. Vienna, Austria. `http://www.R-project.org/`.

Rothery, P. and Roy, D. B. (2001), "Application of generalized additive models to butterfly transect count data", *Journal of Applied Statistics*, 28, 897–909.

Roy, D. B., Rothery, P., Moss, D., Pollard, E. and Thomas, J. A. (2001), "Butterfly numbers and weather: predicting historical trends in abundance and the future effects of climate change", *Journal of Animal Ecology*, 70, 201–217.

Roy, D. B. and Sparks, T. H. (2000), "Phenology of British butterflies and climate change", *Global Change Biology*, 6, 407–416.

Soulsby, R. L. and Thomas, J. A. (2012), "Insect population curves: modelling and application to butterfly transect data", *Methods in Ecology and Evolution*, 3, 832–841.

Sparks, T. H. and Yates, T. J. (1997), "The effect of spring temperature on the appearance

dates of British butterflies 1883–1993", *Ecography*, 20, 368–374.

Spieth, H. R., Pörschmann, U. and Teiwes, C. (2011), "The occurrence of summer diapause in the large white butterfly Pieris brassicae (Lepidoptera: Pieridae): A geographical perspective", *European Journal of Entomology*, 108, 377–384.

Thomas, C. D., Cameron, A., Green, R. E., Bakkenes, M., Beaumont, L. J., Collingham, Y. C., Erasmus, B. F., De Siqueira, M. F., Grainger, A., Hannah, L. et al. (2004), "Extinction risk from climate change", *Nature*, 427, 145–148.

Thomas, J. A. (2005), "Monitoring change in the abundance and distribution of insects using butterflies and other indicator groups", *Philosophical Transactions of the Royal Society B: Biological Sciences*, 360, 339–357.

Van Dyck, H., Bonte, D., Puls, R., Gotthard, K. and Maes, D. (2015), "The lost generation hypothesis: could climate change drive ectotherms into a developmental trap?", *Oikos*, 124, 54–61.

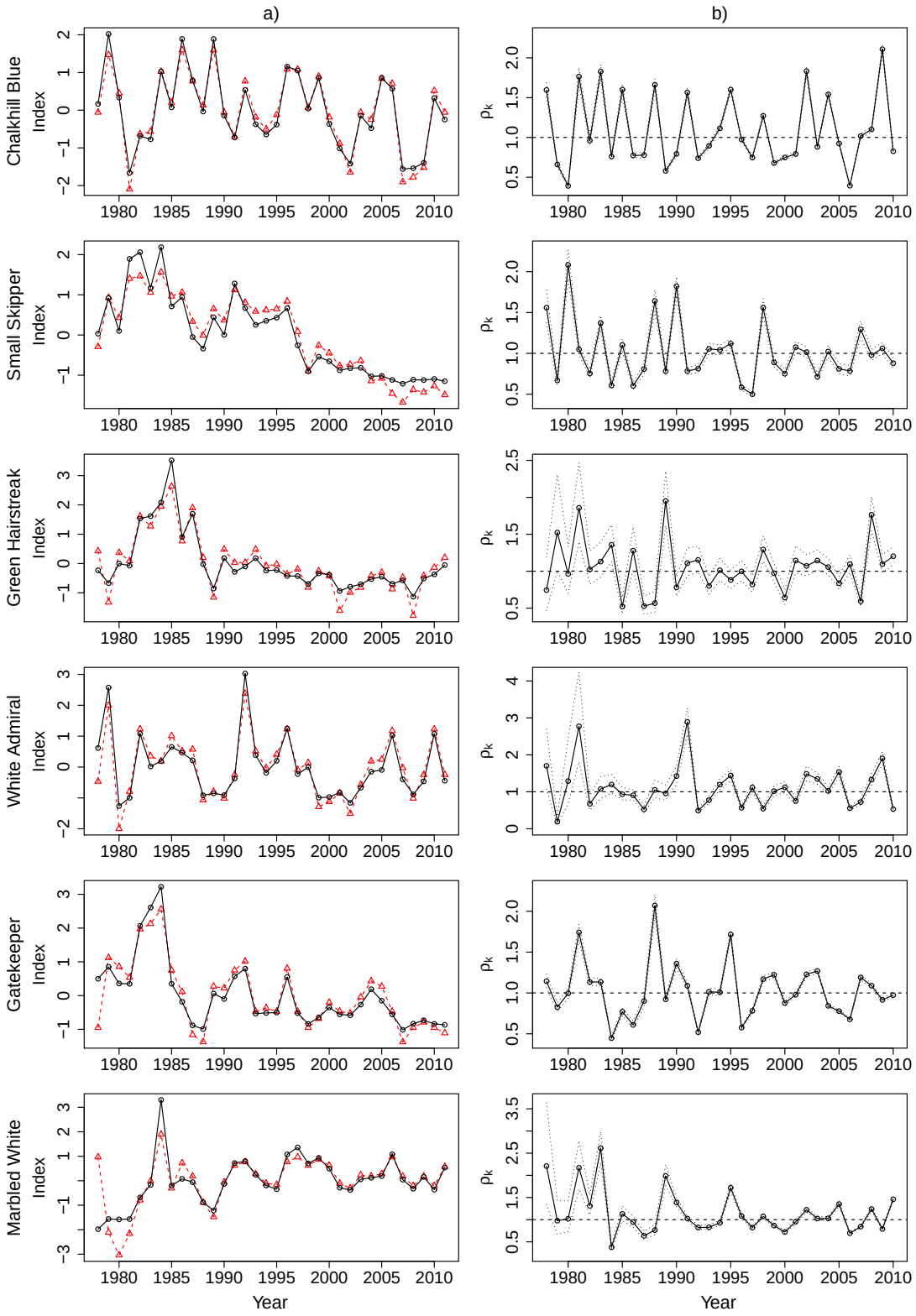

Figure 1: a) Relative abundance indices for each univoltine species from model P_1 (black) and the GAM approach (red) and b) annual estimates of productivity, ρ_k, from model P_1, which was fitted to estimate ρ_k across sites for each year. The horizontal dashed line separates productivities above/below unity, corresponding to growth/decline compared to the previous year. Dotted lines represent 95% confidence intervals for productivity.

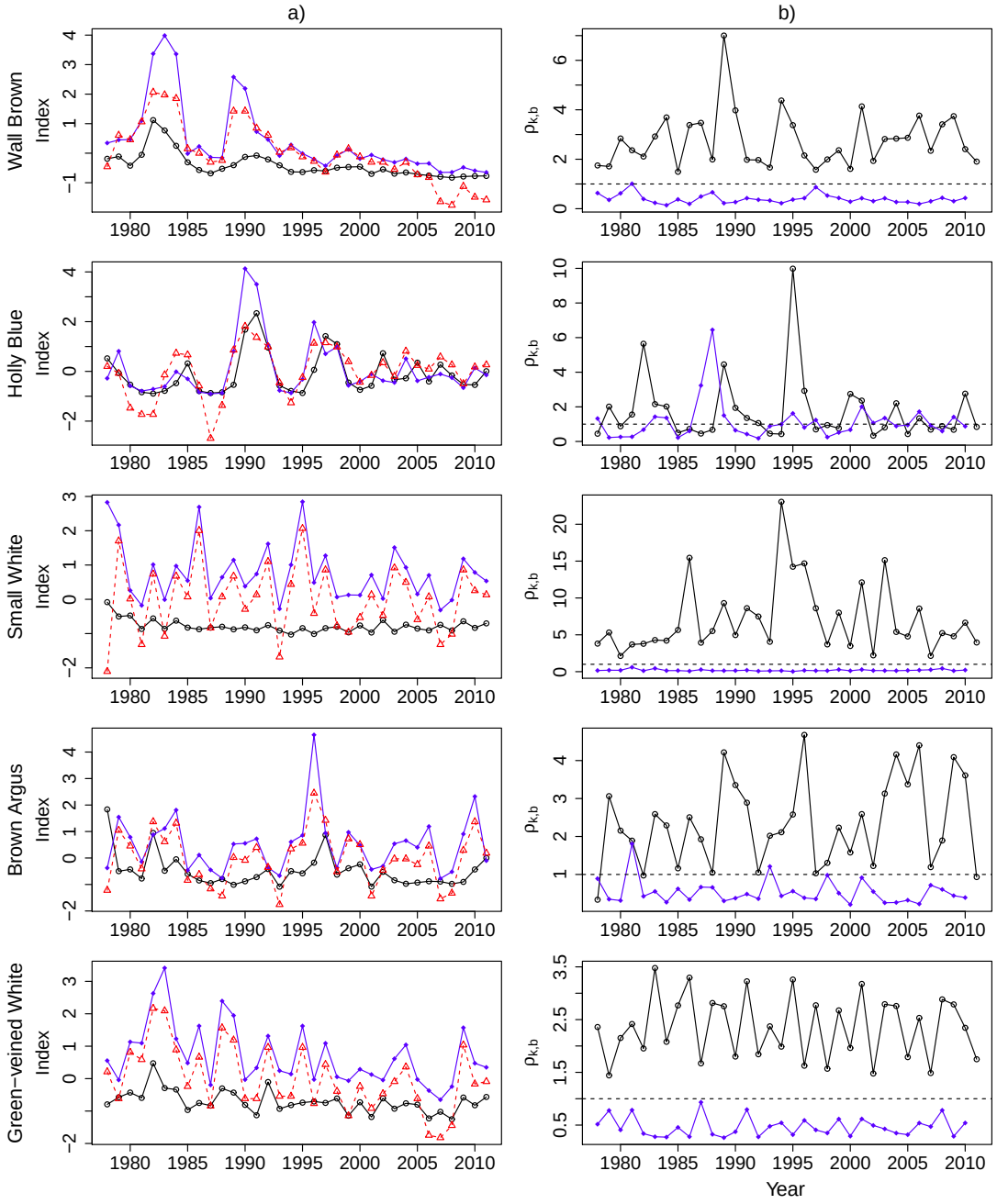

Figure 2: a) Relative abundance indices for each bivoltine species for the first (black) and second (blue) broods from model P_2 and the GAM approach (red) and b) annual estimates of productivity for the first ($\rho_{k,1}$, black) and second ($\rho_{k,2}$, blue) brood from model P_2, which was fitted to estimate $\rho_{k,b}$ across sites for each brood and year. The horizontal dashed line separates productivities above/below unity, corresponding to growth/decline compared to the previous brood.

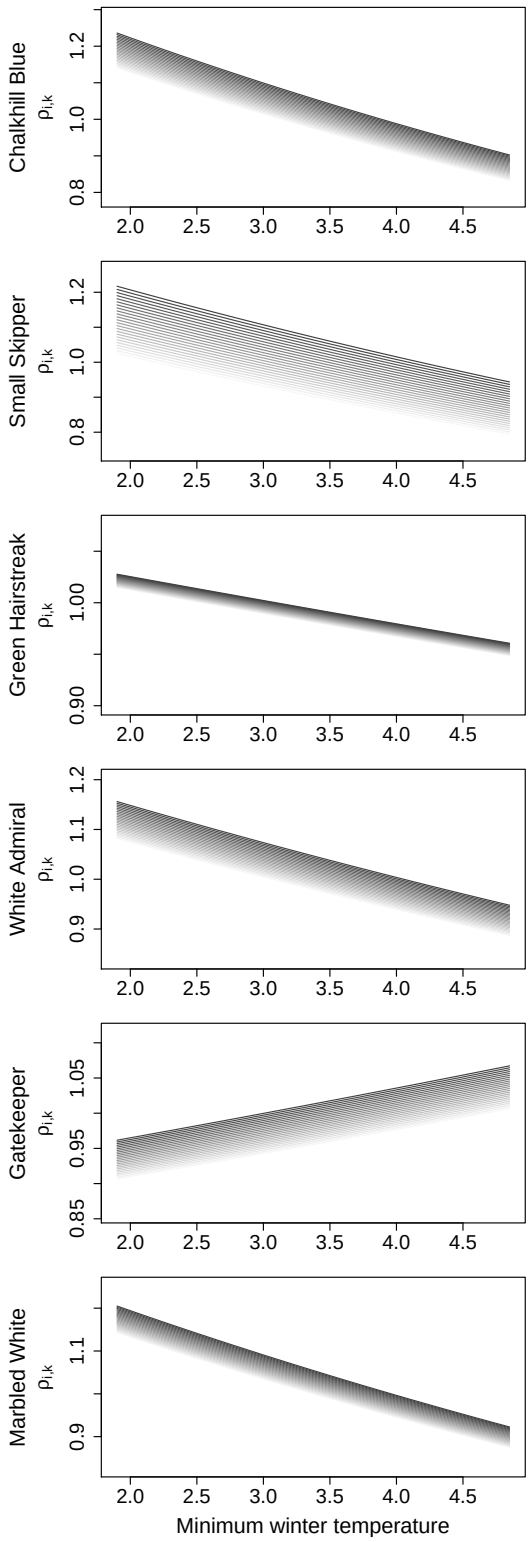

Figure 3: Predicted productivity with varying minimum overwinter temperature from model M_1. Each line represents one of 25 equally-spaced northing values within the species range (red at southern sites and blue at northern sites). Model M_1 was fitted with productivity, $\rho_{i,k}$, and survival probability, $\phi_{i,k}$, regressed on temperature and northing.

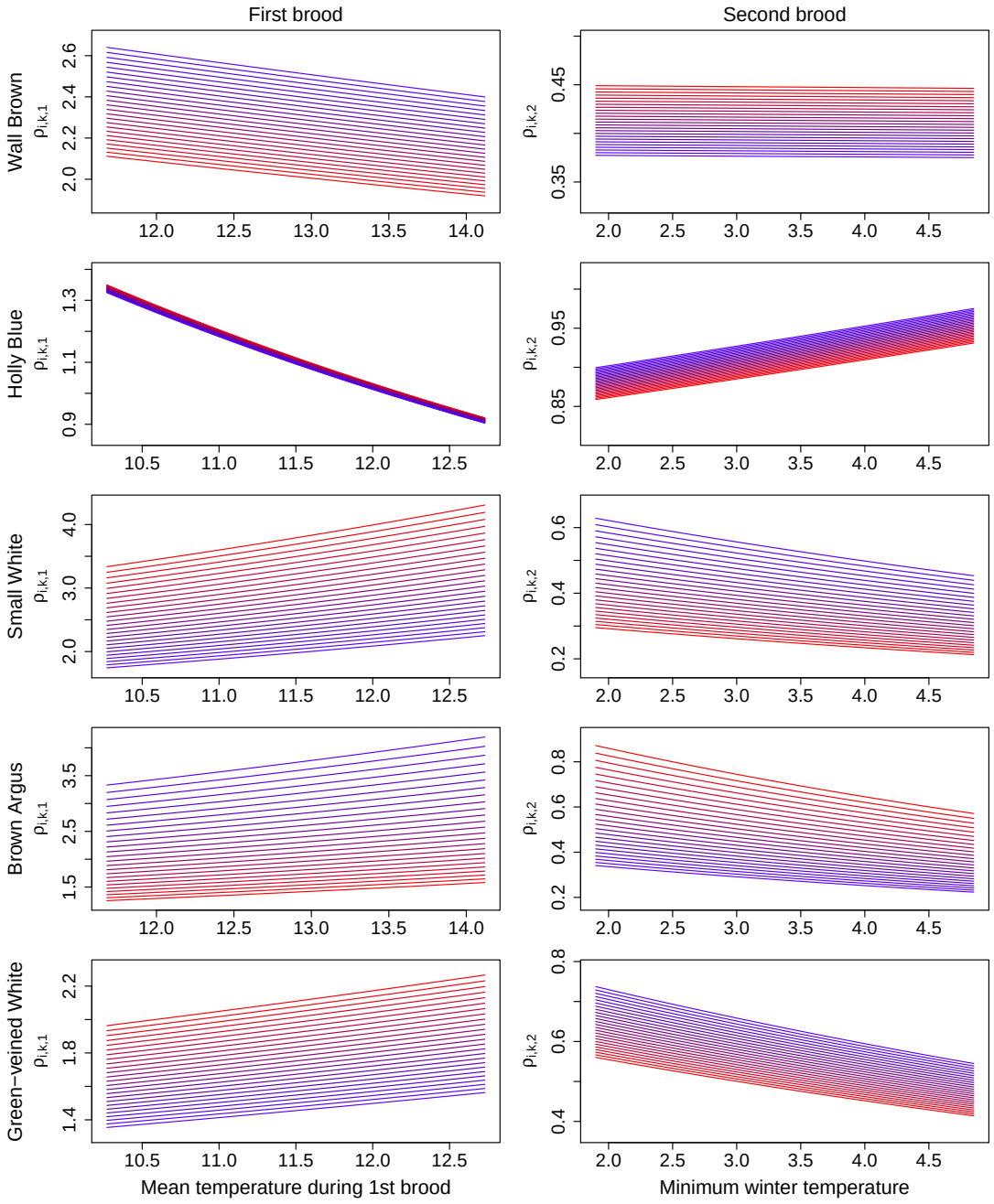

Figure 4: Predicted productivity with varying temperature from model M_2. The mean temperature during the first brood, and the minimum overwinter temperature, were used as covariates for productivity of the first and second brood, respectively. Each line represents one of 25 equally-spaced Northing values within the species range (red at southern sites and blue at northern sites). Model M_2 was fitted with productivity, $\rho_{i,k,b}$, for each brood, b regressed on temperature and northing and survival probability, $\phi_{i,k,b}$, for each brood, b, regressed on temperature.

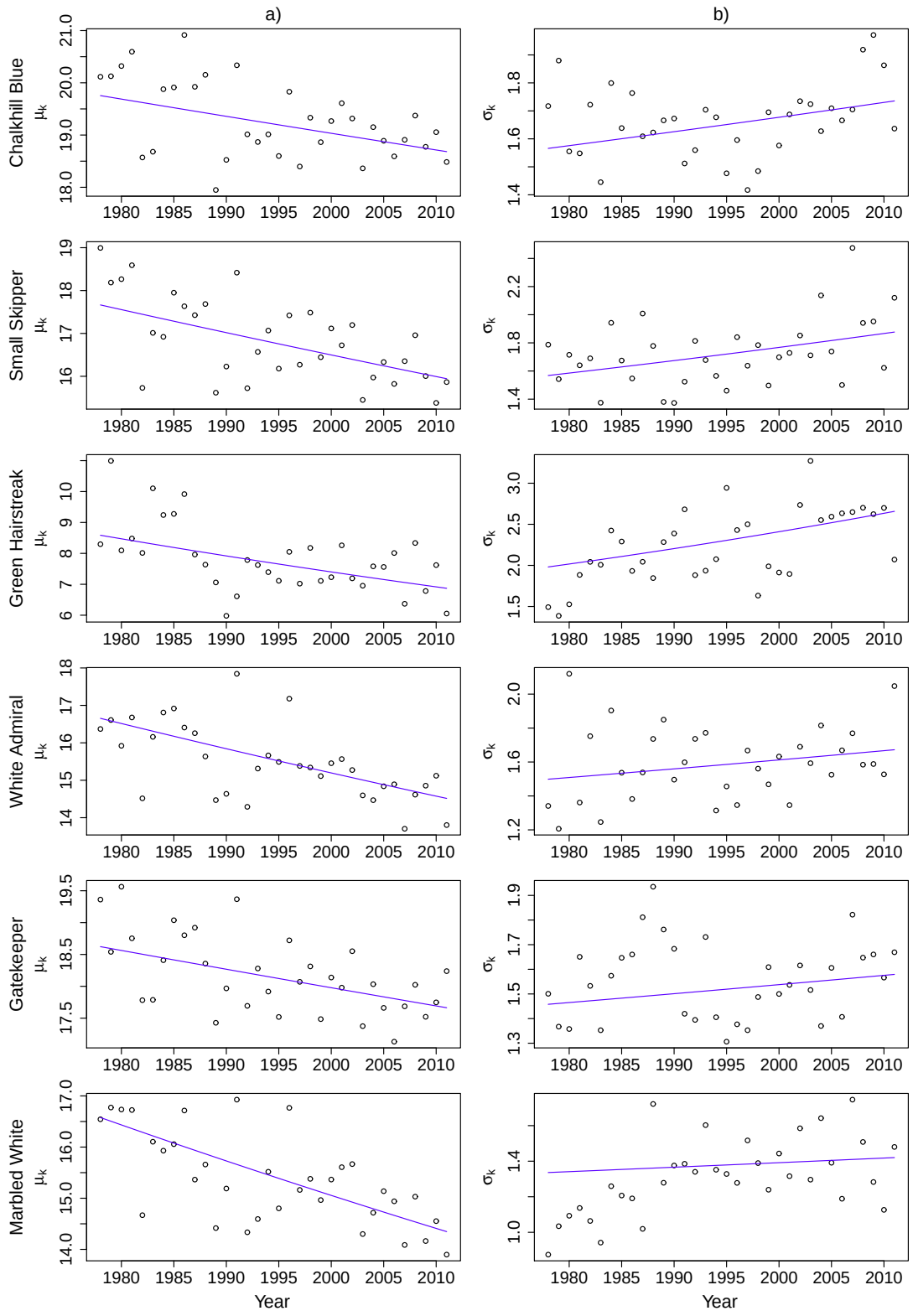

Figure 5: Annual estimates of a) μ_k and b) σ_k from model P_1, which was fitted to estimate ρ_k, μ_k and σ_k across sites for each year. Blue lines indicate fitting log-linear regressions on year for μ and σ, as in Table S2.1a).

Supplementary material:

Dynamic models for longitudinal butterfly data

S1: Additional results and tables for the dynamic models applied to UKBMS data

Table S1.1: Scientific names and approximate flight periods for the sample of butterfly species studied. Approximate flight periods were used for relevant temperature covariates, and specified as the first/last month for which the average weekly count was > 0.1. For bivoltine species, we defined the mid point between the two generations by the month with the minimum weekly count between the two peaks in counts, and hence assumed the break between two generations to always be less than one month.

Common name	Scientific name	Flight period
Chalkhill Blue	*Polyommatus coridon*	July-September
Small Skipper	*Thymelicus sylvestris*	June-September
Green Hairstreak	*Callophrys rubi*	April-July
White Admiral	*Limenitis camilla*	June-August
Gatekeeper	*Pyronia tithonus*	June-September
Marbled White	*Melanargia galathea*	June-August
Wall Brown	*Lasiommata megera*	April-July-September
Holly Blue	*Celastrina argiolus*	April-June-September
Small White	*Pieris rapae*	April-June-September
Brown Argus	*Aricia agestis*	April-July-September
Green-veined White	*Pieris napi*	April-June-September

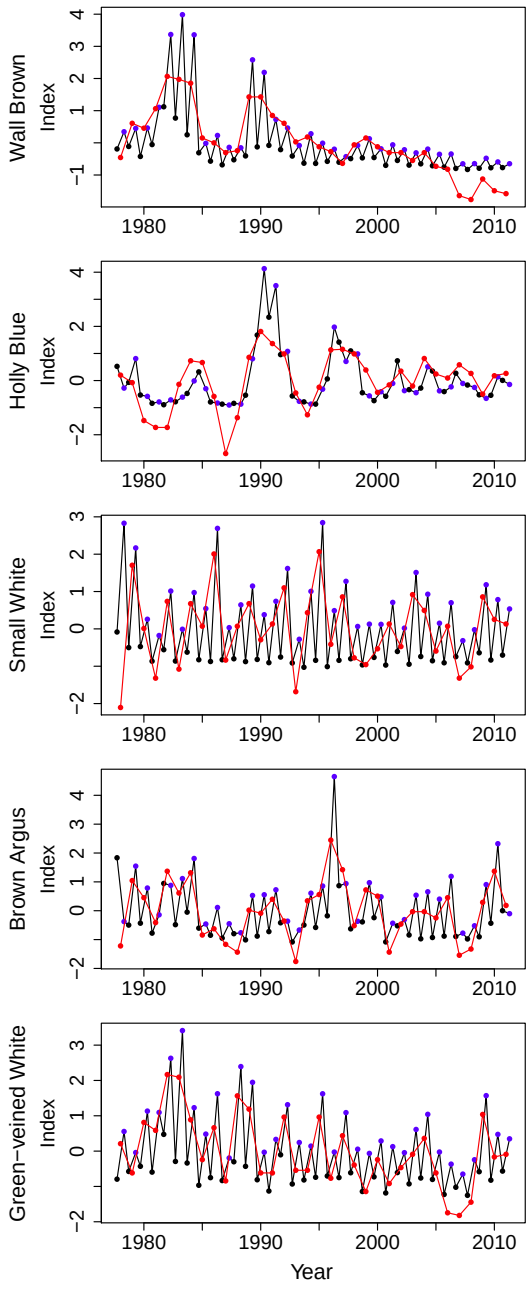

Figure S1.1: Alternative representation of relative abundance indices for the first (black circles) and second (blue) broods from model P_2 and the GAM approach (red).

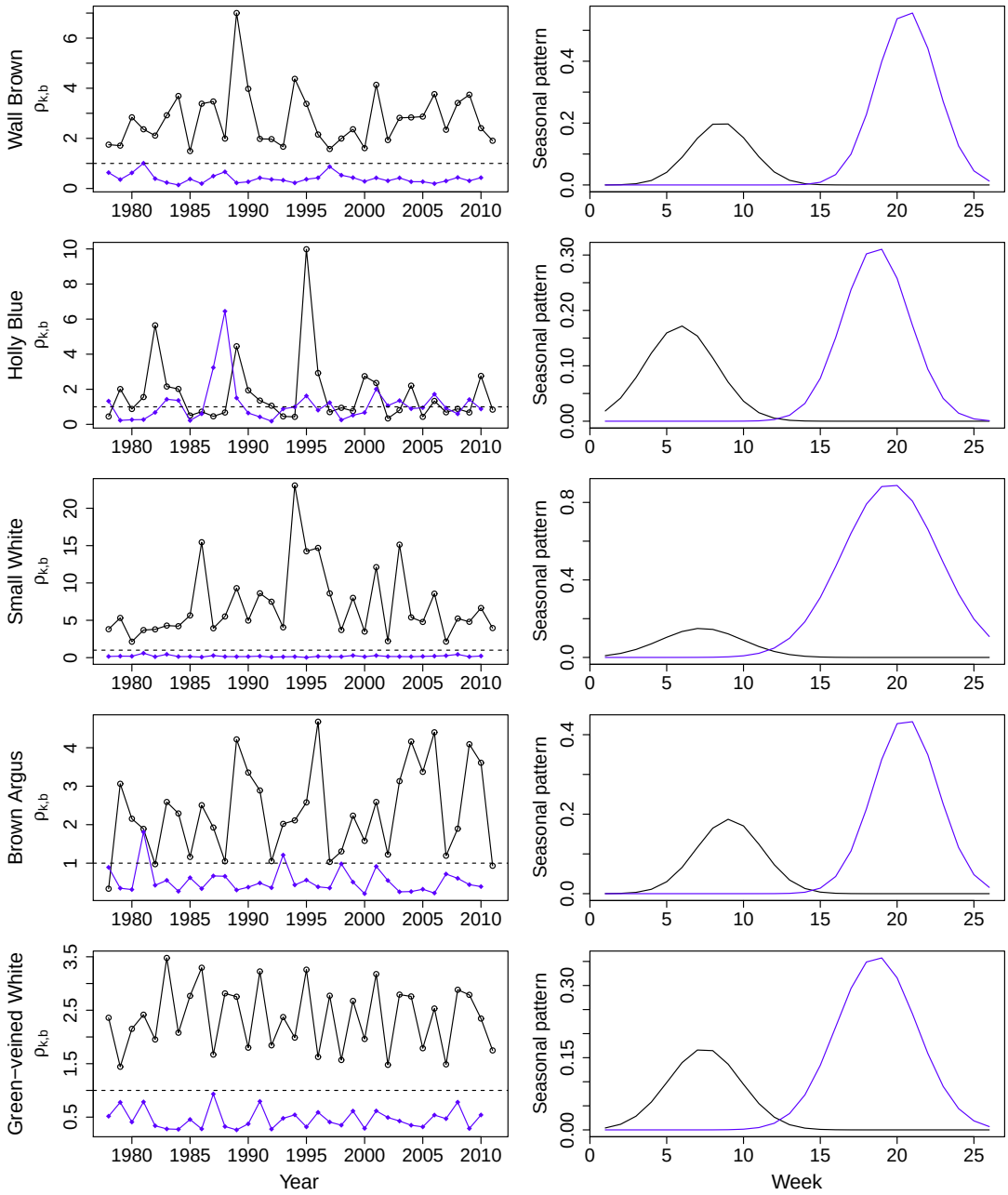

Figure S1.2: a) Annual estimates of productivity for the first ($\rho_{k,1}$, black open circles) and second ($\rho_{k,2}$, blue closed diamonds) brood for each bivoltine species. Model P_2 was fitted to estimate $\rho_{k,b}$ across sites for each brood and year. The horizontal dashed line separates productivities above/below unity, corresponding to growth/decline compared to the previous brood. b) The corresponding average seasonal patterns.

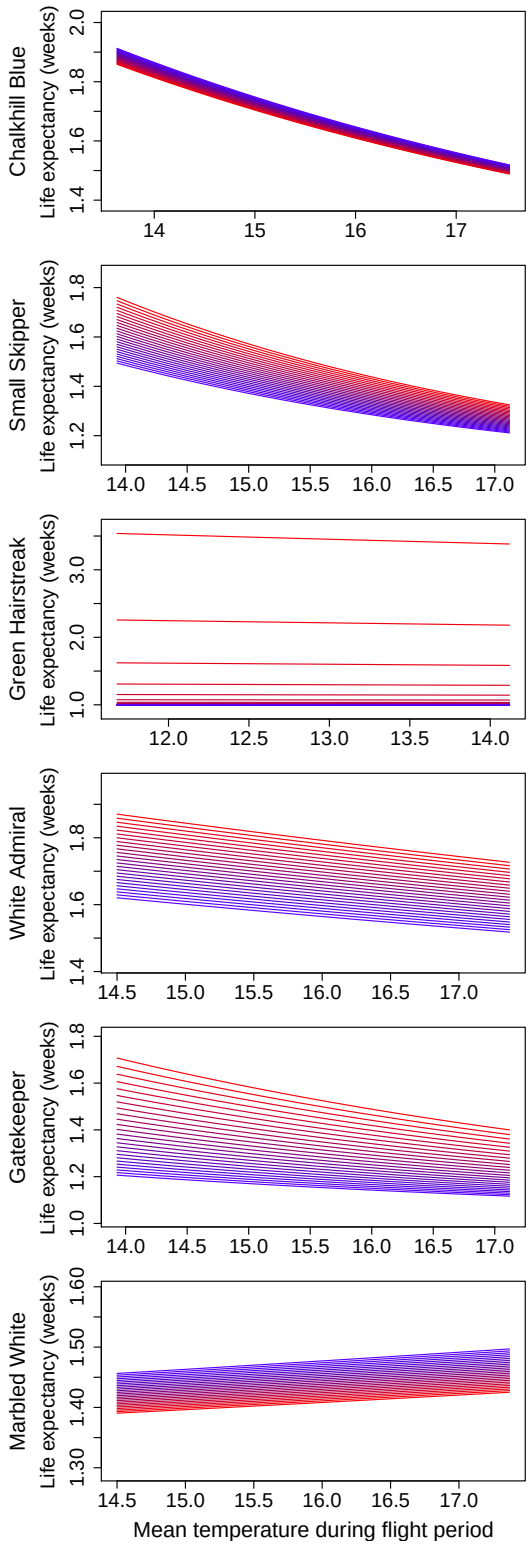

Figure S1.3: Predicted life expectancy (in weeks) with varying temperature from model M_1. Each line represents one of 25 equally-spaced Northing values within the species range (red at southern sites and blue at northern sites). Model M_1 was fitted with $\rho_{i,k}$ and $\phi_{i,k}$ regressed on temperature and northing.

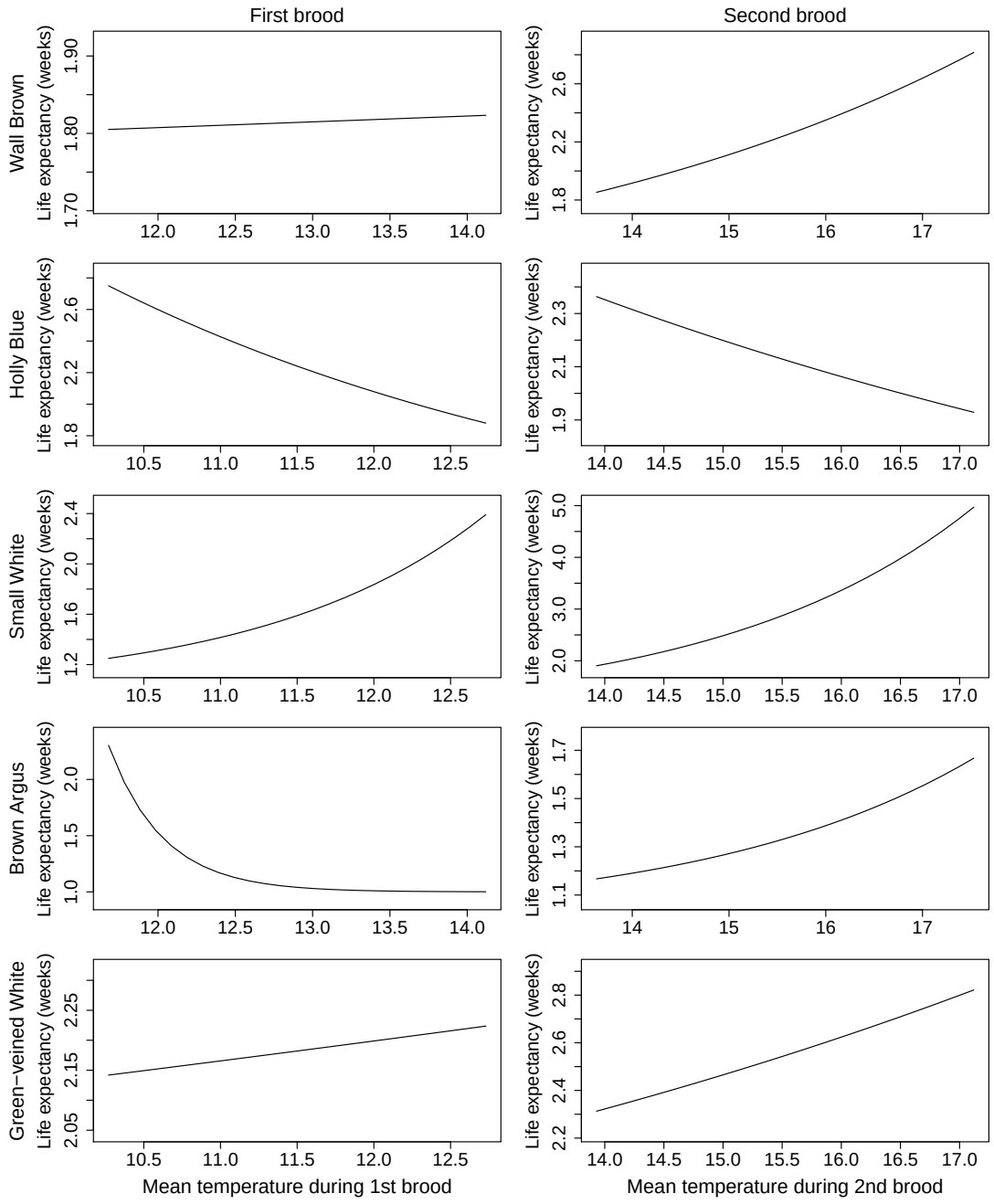

Figure S1.4: Predicted life expectancy for each brood (in weeks) with varying temperature from model M_2. Model M_2 was fitted with $\rho_{i,k,b}$ for each brood regressed on temperature and northing and $\phi_{i,k,b}$ for each brood regressed on temperature.

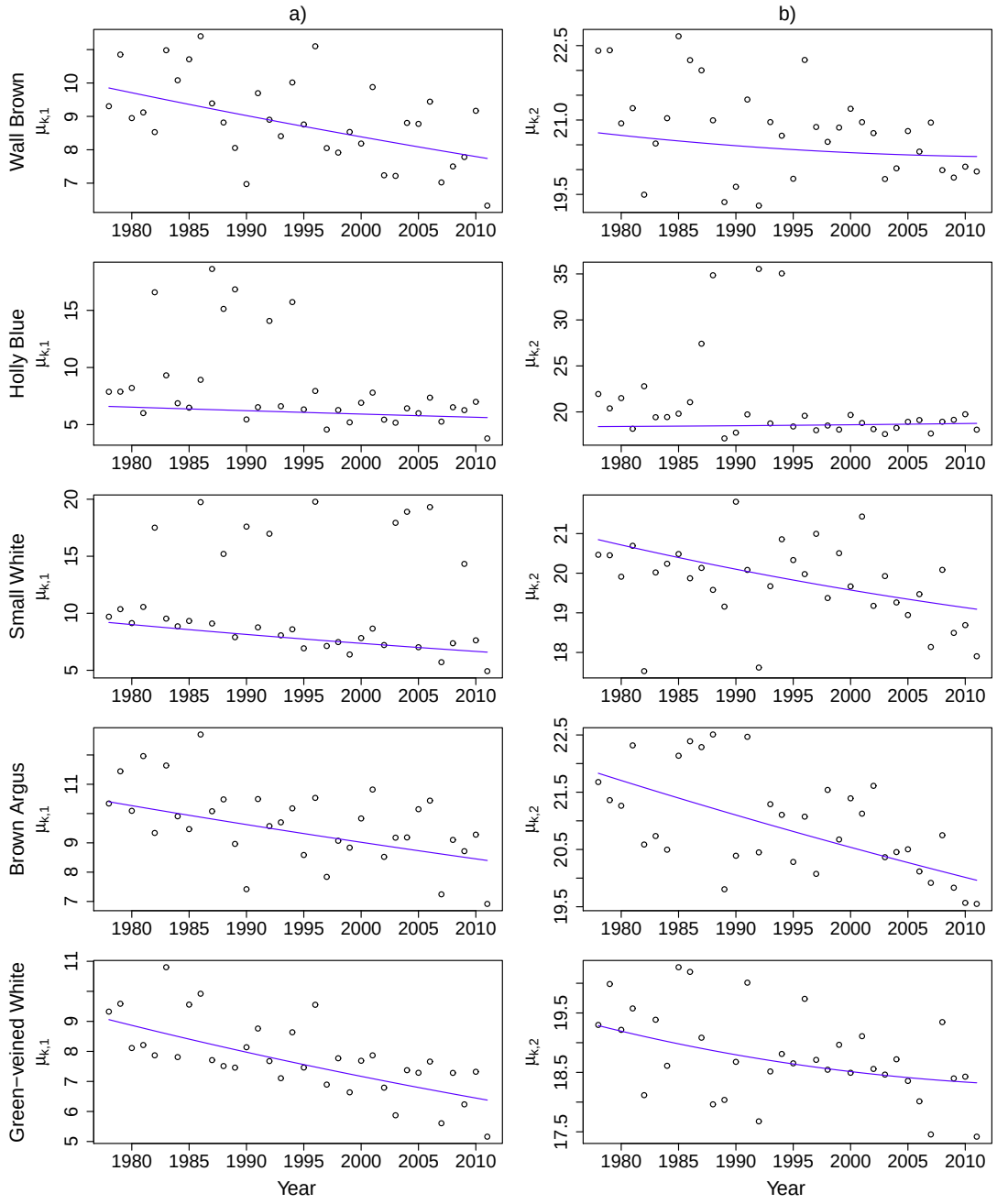

Figure S1.5: Annual estimates of a) $\mu_{k,1}$ and b) $\mu_{k,2}$ from model P_2, which was fitted to estimate $\rho_{k,b}$, $\mu_{k,b}$ and $\sigma_{k,b}$ across sites for each brood and year. Blue lines indicate fitting log-linear regressions on year for μ for each brood.

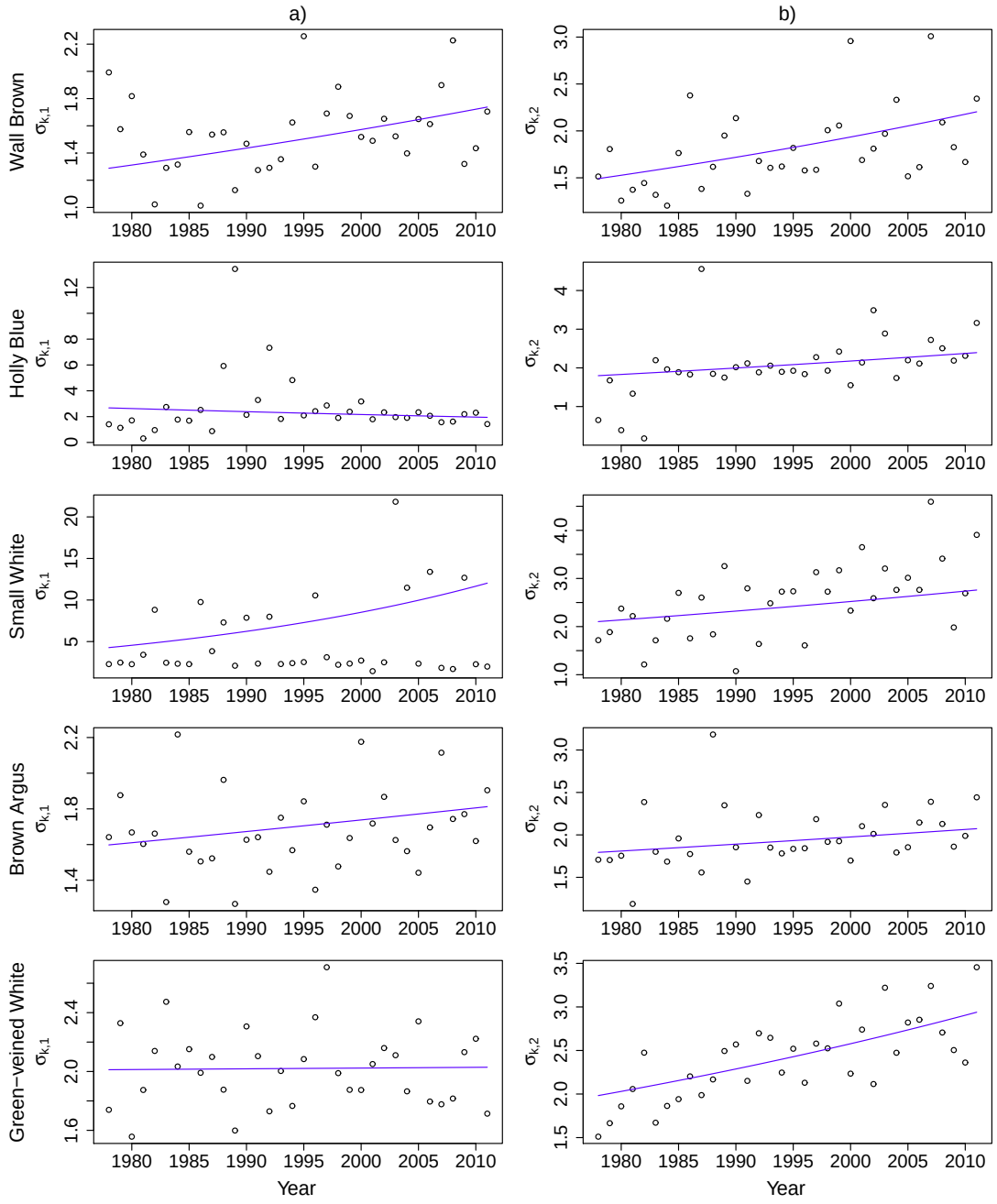

Figure S1.6: Annual estimates of a) $\sigma_{k,1}$ and b) $\sigma_{k,2}$ from model P_2, which was fitted to estimate $\rho_{k,b}$, $\mu_{k,b}$ and $\sigma_{k,b}$ across sites for each brood and year. Blue lines indicate fitting log-linear regressions on year for σ for each brood.

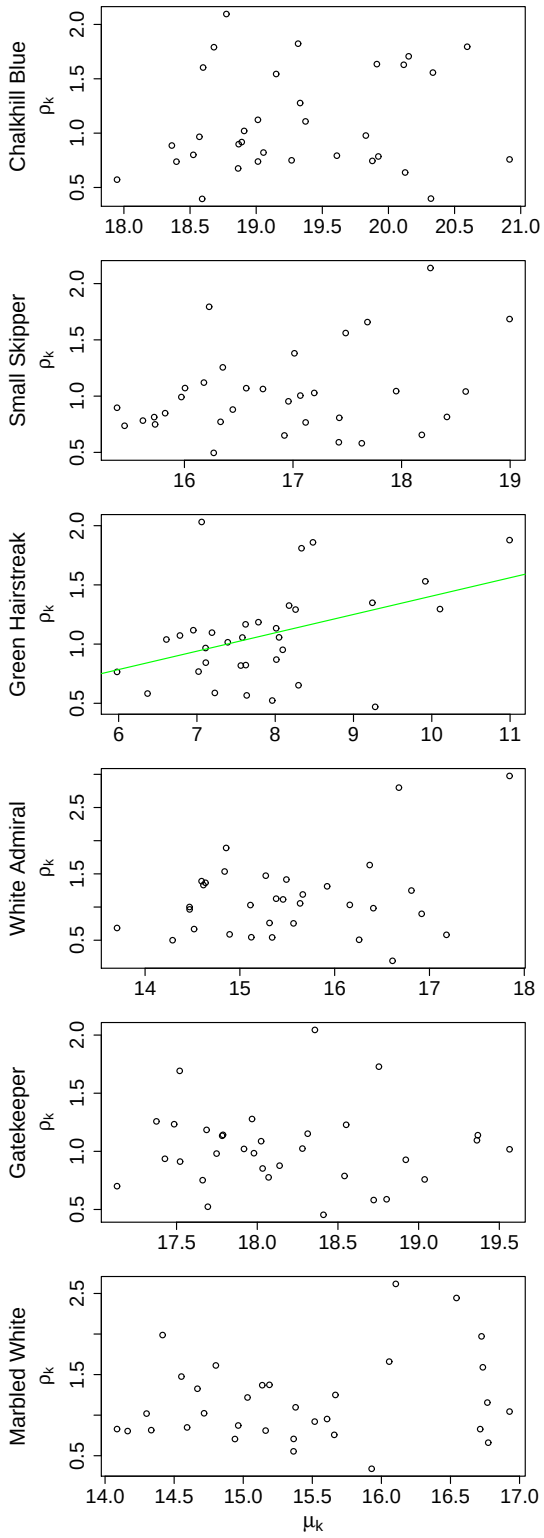

Figure S1.7: Annual estimates of μ_k versus productivity ρ_k from model P_1, which was fitted to estimate ρ_k, μ_k and σ_k across sites for each year. The green line indicates a significant trend based on performing a simple linear regression post-model fitting.

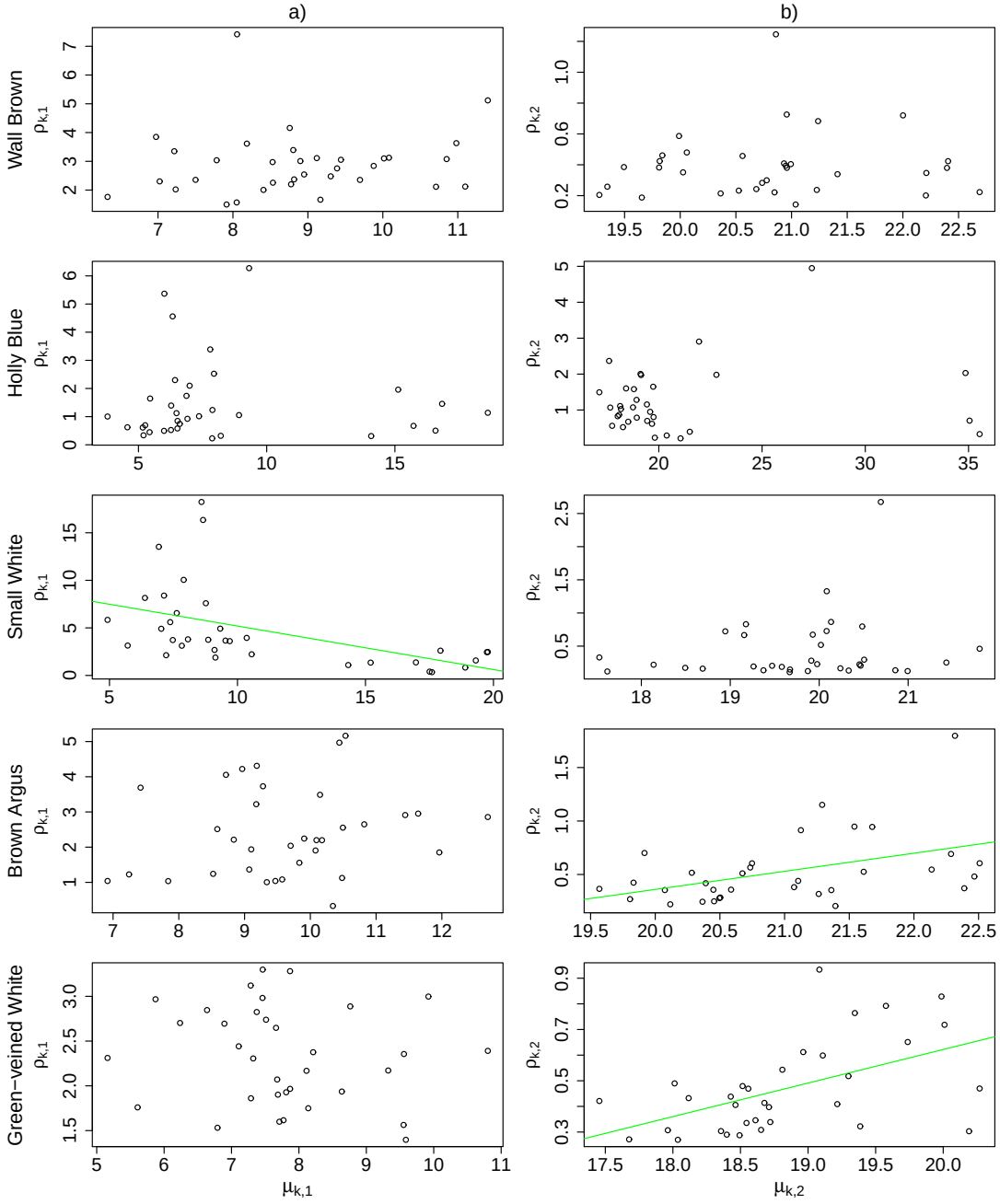

Figure S1.8: Annual estimates of a) $\mu_{k,1}$ versus $\rho_{k,1}$ and b) $\mu_{k,2}$ versus $\rho_{k,2}$ from model P_2, which was fitted to estimate $\rho_{k,b}$, $\mu_{k,b}$ and $\sigma_{k,b}$ across sites for each brood and year. Green lines indicate a significant trend based on performing a simple linear regression post-model fitting.

Table S1.2: Parameter estimates from the a) M_1 and b) P_1 models. Est and SE represent the parameter estimate and standard error, respectively. All estimates are on the log scale, except those relating to ϕ which are on the logit scale.

		Chalkhill Blue		Small Skipper		Green Hairstreak		White Admiral		Gatekeeper		Marbled White	
	Parameter	Est	SE	Est	SE	Est	SE	Est	SE	Est	SE	Est	SE
a)	$\rho_{i,k}$(intercept)	0.0194	0.0004	-0.0455	0.0008	-0.0140	0.0023	0.0094	0.0025	-0.0365	0.0005	0.0255	0.0011
	$\rho_{i,k}$(wtemp)	-0.0772	0.0011	-0.0624	0.0021	-0.0165	0.0056	-0.0487	0.0059	0.0256	0.0012	-0.0655	0.0023
	$\rho_{i,k}$(northing)	0.0199	0.0004	0.0399	0.0010	0.0029	0.0016	0.0158	0.0015	0.0108	0.0003	0.0107	0.0009
	$\phi_{i,k}$(intercept)	-0.4161	0.0109	-0.7725	0.0423	-2.3267	0.2276	-0.3347	0.0399	-0.9194	0.0175	-0.8585	0.0234
	$\phi_{i,k}$(temp)	-0.1246	0.0038	-0.1893	0.0107	-0.0155	0.0205	-0.0513	0.0151	-0.1270	0.0054	0.0242	0.0075
	$\phi_{i,k}$(northing)	0.0145	0.0056	-0.0960	0.0214	-3.8071	0.3083	-0.0776	0.0220	-0.2185	0.0087	0.0304	0.0128
	μ(emergence)	2.8857	0.0004	2.7588	0.0013	1.8340	0.0048	2.6408	0.0021	2.8375	0.0004	2.6362	0.0007
	σ(emergence)	0.3704	0.0028	0.5488	0.0060	0.7506	0.0090	0.4023	0.0120	0.3391	0.0028	0.2842	0.0046
b)	$\rho_{i,k}$(intercept)	0.0192	0.0004	-0.0472	0.0008	-0.0151	0.0023	0.0092	0.0025	-0.0377	0.0005	0.0256	0.0011
	$\rho_{i,k}$(wtemp)	-0.0763	0.0011	-0.0662	0.0021	-0.0157	0.0056	-0.0492	0.0059	0.0270	0.0012	-0.0660	0.0023
	$\rho_{i,k}$(northing)	0.0209	0.0004	0.0410	0.0010	0.0037	0.0016	0.0158	0.0015	0.0109	0.0003	0.0109	0.0009
	μ(flight period)	2.9473	0.0002	2.8188	0.0005	2.0007	0.0033	2.7227	0.0010	2.8892	0.0002	2.7001	0.0003
	σ(flight period)	0.5797	0.0013	0.6690	0.0029	0.9534	0.0071	0.6291	0.0056	0.4834	0.0014	0.4458	0.0022

Table S1.3: Parameter estimates from the a) M_2 and b) P_2 models. Est and SE represent the parameter estimate and standard error, respectively. All estimates are on the log scale, except those relating to ϕ which are on the logit scale.

		Wall Brown		Holly Blue		Small White		Brown Argus		Green-veined White	
	Parameter	Est	SE	Est	SE	Est	SE	Est	SE	Est	SE
a)	$\rho_{i,k,1}$(intercept)	0.7869	0.0436	0.1003	0.0755	1.1730	0.1016	0.6211	0.0474	0.6392	0.0415
	$\rho_{i,k,1}$(temp)	-0.0234	0.0048	-0.1089	0.0068	0.0727	0.0022	0.0564	0.0033	0.0408	0.0018
	$\rho_{i,k,1}$(north)	0.0674	0.0175	-0.0038	0.0284	-0.1312	0.0138	0.1596	0.0153	-0.1012	0.0088
	$\rho_{i,k,2}$(intercept)	-0.8674	0.0436	-0.1021	0.0756	-1.1815	0.1017	-0.6095	0.0475	-0.6374	0.0416
	$\rho_{i,k,2}$(wtemp)	-0.0015	0.0059	0.0198	0.0102	-0.0801	0.0032	-0.1037	0.0049	-0.0742	0.0026
	$\rho_{i,k,2}$(north)	-0.0524	0.0176	0.0094	0.0285	0.1529	0.0138	-0.1537	0.0154	0.0748	0.0089
	$\phi_{i,k,1}$(intercept)	-0.2068	0.0940	0.2106	0.1182	-0.5156	0.3086	-2.8444	0.6983	0.1678	0.0888
	$\phi_{i,k,1}$(temp)	0.0055	0.0239	-0.1956	0.0334	0.4891	0.0701	-1.7035	0.4374	0.0197	0.0136
	$\phi_{i,k,2}$(intercept)	0.2277	0.0121	0.1430	0.0265	0.5430	0.0086	-1.0809	0.0296	0.4148	0.0064
	$\phi_{i,k,2}$(temp)	0.1667	0.0327	-0.0855	0.0918	0.3297	0.0559	0.3056	0.1391	0.0730	0.0234
	μ_1(emergence)	2.0203	0.0090	1.4842	0.0271	1.8331	0.0243	2.1331	0.0046	1.8044	0.0124
	μ_d(emergence)	2.4234	0.0063	2.5370	0.0115	2.4170	0.0141	2.4201	0.0054	2.3789	0.0073
	σ_1(emergence)	0.5647	0.0207	0.6306	0.0380	0.9677	0.0182	0.7065	0.0105	0.7482	0.0166
	σ_2(emergence)	0.3105	0.0159	0.5797	0.0333	0.9116	0.0170	0.6887	0.0098	0.6179	0.0119
b)	$\rho_{i,k,1}$(intercept)	-1.0292	0.0176	-0.1019	0.0243	-1.7222	0.0129	-0.8385	0.0143	-0.8373	0.0084
	$\rho_{i,k,1}$(temp)	-0.0447	0.0053	-0.0985	0.0066	0.0470	0.0021	0.0643	0.0032	0.0374	0.0018
	$\rho_{i,k,1}$(north)	0.0591	0.0153	-0.0130	0.0282	-0.1257	0.0141	0.1605	0.0153	-0.1017	0.0088
	$\rho_{i,k,2}$(intercept)	0.9542	0.0177	0.0968	0.0245	1.7188	0.0129	0.8466	0.0144	0.8396	0.0084
	$\rho_{i,k,2}$(wtemp)	0.0326	0.0069	0.0113	0.0101	-0.0604	0.0031	-0.1090	0.0045	-0.0703	0.0025
	$\rho_{i,k,2}$(north)	-0.0664	0.0154	0.0187	0.0282	0.1459	0.0142	-0.1544	0.0153	0.0752	0.0088
	μ_1(flight period)	2.1423	0.0034	1.7744	0.0078	1.9703	0.0047	2.2037	0.0026	2.0105	0.0023
	μ_d(flight period)	2.4924	0.0028	2.5391	0.0047	2.5157	0.0029	2.4419	0.0024	2.4152	0.0018
	σ_1(flight period)	0.6731	0.0109	0.8727	0.0157	0.9510	0.0113	0.7457	0.0084	0.8616	0.0061
	σ_2(flight period)	0.6640	0.0067	0.8497	0.0130	1.1478	0.0044	0.7496	0.0057	0.9529	0.0038

S2: Comparison with the GAI approach

The GAI approach is more general than the dynamic models. GAI models provide a broad framework for modelling butterfly count data for any given year, encompassing a range of possible discrete distributions as well as phenomenological, stopover and spline alternatives for modelling.

In Table S2.1 we compare estimates of μ_k and σ_k from model P_1 and the GAI approach (Dennis et al. 2014). The GAI models have structural similarities to the dynamic models, but do not link abundance from different years separately, and hence unlike the dynamic models do not provide estimates of productivity. Here we fitted the $\mathrm{P/N}_1$ model, which assumes a Poisson distribution, with Normal, $N(\mu, \sigma^2)$, probability density for describing seasonal variation in the counts. We regressed μ and σ on year on the log scale, therefore for the GAI we fitted a joint likelihood for multiple years, where there were four parameters to estimate. Model P_1 was also fitted with μ and σ regressed on year, with the addition of annual estimates for productivity, compared with the GAI.

The estimates and associated standard errors from the two models are similar. The estimates of dispersion of Table S2.1 suggest overdispersion in some cases, requiring attention, e.g. by suitably inflating standard errors. Figure S2.1 demonstrates positive correlation in estimates of site abundance from the two methods.

Indices of abundance from the dynamic model and GAI show good agreement with the index resulting from the GAM approach (Dennis et al. 2013) in Figure S2.2. The index from the dynamic model is often closer to the GAM index than the GAI is, for example in some years for Gatekeeper and Marbled White. This could be a result of variation in the set of sites monitored each year, which is accounted for by the GAM approach, as well as in the dynamic model, where N (Section 2.5) can be estimated for every site for each year (and brood where appropriate). In contrast, for the GAI only sites visited in a given year contribute to the estimated index.

On average across the six species, the GAI took 12 seconds, whereas the dynamic model

took 87 minutes. Since differences between the indices produced from different methods are fairly small, the GAI may be better suited to estimating indices of abundance, whereas the dynamic model can provide estimates of productivity, as well as separate indices and survival probabilities for different broods, but with greater computational requirements.

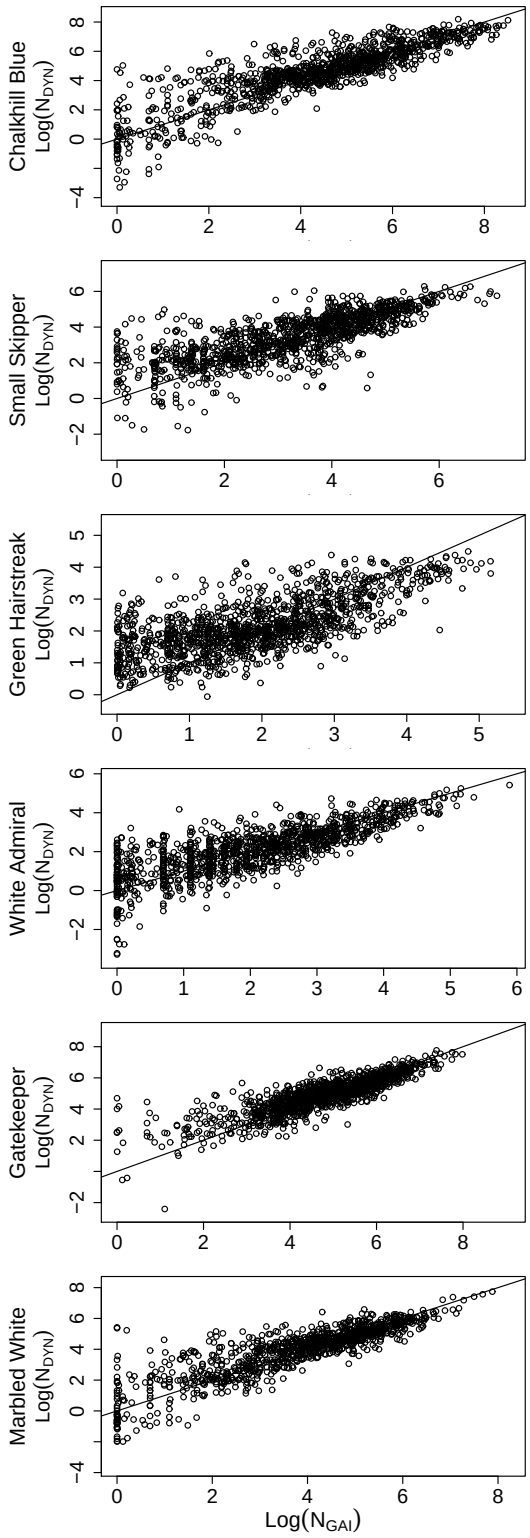

Figure S2.1: Comparison of site parameters $\{N_{ik}\}$ from the P/N$_1$ GAI model (N$_{\mathrm{GAI}}$) and model P$_1$ (N$_{\mathrm{DYN}}$), as fitted in Table S2.1. Both axes are displayed on the log scale and the line indicates the 1-1 line.

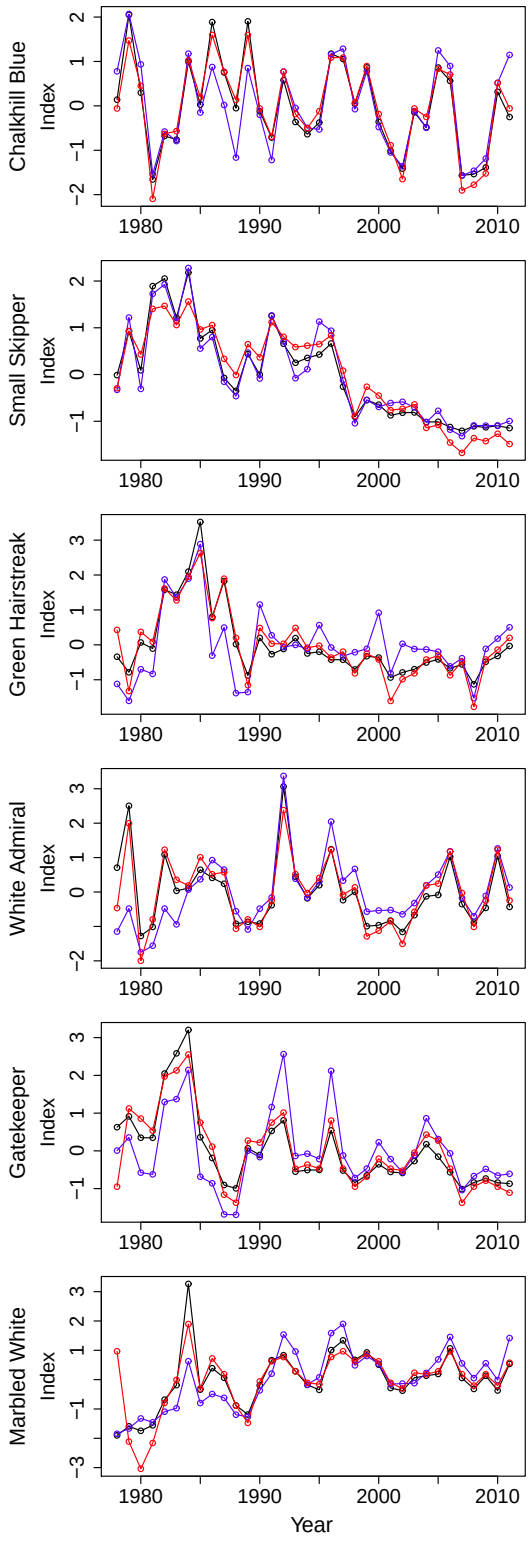

Figure S2.2: Relative abundance indices from dynamic model P_1 (black), the P/N_1 GAI model (blue) and the GAM approach (red). The GAM approach is as fitted in Section 3.1. The dynamic and GAI models are as fitted in Table S2.1.

Table S2.1: Comparison of a) P_1 model and b) GAI model P/N_1 with log-linear regressions on year. Est and SE represent the parameter estimate and associated standard error, respectively. All estimates are on the log scale. To reduce bias, estimates for σ are based on models with time-varying μ. D is the dispersion (residual deviance/degrees of freedom) and T is the approximate computation time in minutes, based on models with log-linear regressions on year.

	Species	μ_k(int)		μ_k(slope)		σ_k(int)		σ_k(slope)		D	T
		Est	SE	Est	SE	Est	SE	Est	SE		
a)	Chalkhill Blue	2.9555	0.0002	-0.0168	0.0002	0.4999	0.0013	0.0310	0.0020	9.4	91
	Small Skipper	2.8203	0.0005	-0.0309	0.0005	0.5397	0.0031	0.0542	0.0020	3.3	57
	Green Hairstreak	2.0387	0.0034	-0.0673	0.0037	0.8305	0.0275	0.0886	0.0296	1.1	35
	White Admiral	2.7439	0.0011	-0.0415	0.0012	0.4594	0.0256	0.0331	0.0172	0.8	120
	Gatekeeper	2.8980	0.0002	-0.0159	0.0002	0.4170	0.0018	0.0241	0.0018	6.5	72
	Marbled White	2.7358	0.0005	-0.0436	0.0005	0.3203	0.0114	0.0184	0.0081	4.2	147
b)	Chalkhill Blue	2.9557	0.0002	-0.0169	0.0002	0.5015	0.0014	0.0298	0.0020	4.6	0.21
	Small Skipper	2.8199	0.0005	-0.0313	0.0005	0.5372	0.0031	0.0559	0.0020	1.9	0.24
	Green Hairstreak	2.0408	0.0035	-0.0673	0.0037	0.8311	0.0278	0.0881	0.0305	0.8	0.14
	White Admiral	2.7448	0.0011	-0.0413	0.0012	0.4606	0.0261	0.0313	0.0173	0.6	0.22
	Gatekeeper	2.8980	0.0002	-0.0159	0.0002	0.4152	0.0018	0.0255	0.0018	4.5	0.21
	Marbled White	2.7359	0.0005	-0.0436	0.0005	0.3199	0.0118	0.0202	0.0080	3.0	0.24

S3: Summary of results from the dynamic models applied to simulated data

Data were simulated based on $T = 25$, $Y = 5$ and $S = 50$ (except for the M_2 model where we set $S = 100$). The parameter values used are given in Tables S3.1 and S3.2. For each of 100 simulated data sets, the initial site abundance parameters, $\{N_{i,1,1}\}$, were simulated from a Poisson distribution with expectation of 150, and were used in combination with the productivity parameters to produce site abundance values for consecutive broods and years. The fitted models produce precise estimates of the true parameter values for the univoltine models, with an increase in variability for more complex bivoltine models, particularly the M_2 model which produced less precise and slightly biased parameter estimates, at least for a survey of this scale.

Table S3.1: Summary of output from 100 simulations for the a) P_1 and b) M_1 dynamic model. Data were simulated for $Y = 5$ years and $S = 50$ sites. The mean is the mean estimate of the parameter from 100 simulations. SE and RMSE are the associated standard error and root-mean-square error, respectively.

	Parameter	True value	Mean	SE	RMSE
a)	ρ_1	0.75	0.75	0.002	0.023
	ρ_2	1.00	1.01	0.003	0.033
	ρ_3	1.25	1.24	0.004	0.043
	ρ_4	1.50	1.51	0.004	0.041
	μ	10.00	10.00	0.003	0.027
	σ	3.00	3.00	0.002	0.019
b)	ρ_1	0.75	0.75	0.001	0.012
	ρ_2	1.00	1.00	0.002	0.020
	ρ_3	1.25	1.25	0.002	0.025
	ρ_4	1.50	1.50	0.003	0.026
	μ	10.00	10.00	0.009	0.093
	σ	3.00	3.00	0.003	0.027
	ϕ	0.25	0.25	0.006	0.057

Table S3.2: Summary of output from 100 simulations for the a) P_2 and b) M_2 dynamic model. Data were simulated for $Y = 5$ years and $S = 50$ and $S = 100$ sites for the P_2 and M_2 models, respectively. The mean is the mean estimate of the parameter from 100 simulations. SE and RMSE are the associated standard error and root-mean-square error, respectively.

	Parameter	True value	Mean	SE	RMSE
a)	$\rho_{1,1}$	0.90	0.91	0.003	0.033
	$\rho_{2,1}$	0.85	0.85	0.003	0.028
	$\rho_{3,1}$	0.80	0.80	0.003	0.027
	$\rho_{4,1}$	0.75	0.75	0.002	0.023
	$\rho_{5,1}$	0.70	0.70	0.002	0.021
	$\rho_{1,2}$	1.25	1.25	0.004	0.039
	$\rho_{2,2}$	1.42	1.41	0.004	0.042
	$\rho_{3,2}$	1.58	1.59	0.005	0.049
	$\rho_{4,2}$	1.75	1.75	0.005	0.049
	μ_1	10.00	10.00	0.005	0.047
	μ_d	7.00	7.00	0.002	0.021
	σ_1	3.00	3.00	0.003	0.028
	σ_2	2.50	2.50	0.002	0.020
b)	$\rho_{1,1}$	0.90	0.99	0.021	0.222
	$\rho_{2,1}$	0.85	0.93	0.019	0.207
	$\rho_{3,1}$	0.80	0.88	0.018	0.197
	$\rho_{4,1}$	0.75	0.82	0.017	0.180
	$\rho_{5,1}$	0.70	0.77	0.015	0.168
	$\rho_{1,2}$	1.25	1.19	0.026	0.263
	$\rho_{2,2}$	1.42	1.35	0.029	0.296
	$\rho_{3,2}$	1.58	1.51	0.032	0.331
	$\rho_{4,2}$	1.75	1.67	0.036	0.366
	μ_1	10.00	9.91	0.028	0.291
	μ_d	7.00	7.13	0.032	0.344
	σ_1	3.00	2.98	0.005	0.052
	σ_2	2.50	2.51	0.008	0.076
	ϕ_1	0.30	0.32	0.017	0.170
	ϕ_2	0.40	0.38	0.007	0.074